



HAL
open science

N”N”C platinum (II) complexes based on phenyl-pyridin-2-ylpyrimidine ligands: synthesis, electrochemical and photophysical properties

Mariia Hruzd, Sebastien Gauthier, Julien Boixel, Samia Kahlal, Nicolas Le Poul, Jean-Yves Saillard, Sylvain Achelle, Francoise Robin-Le Guen

► To cite this version:

Mariia Hruzd, Sebastien Gauthier, Julien Boixel, Samia Kahlal, Nicolas Le Poul, et al.. N”N”C platinum (II) complexes based on phenyl-pyridin-2-ylpyrimidine ligands: synthesis, electrochemical and photophysical properties. *Dyes and Pigments*, 2021, 194, pp.109622. 10.1016/j.dyepig.2021.109622 . hal-03331329

HAL Id: hal-03331329

<https://hal.science/hal-03331329>

Submitted on 15 May 2023

HAL is a multi-disciplinary open access archive for the deposit and dissemination of scientific research documents, whether they are published or not. The documents may come from teaching and research institutions in France or abroad, or from public or private research centers.

L’archive ouverte pluridisciplinaire **HAL**, est destinée au dépôt et à la diffusion de documents scientifiques de niveau recherche, publiés ou non, émanant des établissements d’enseignement et de recherche français ou étrangers, des laboratoires publics ou privés.

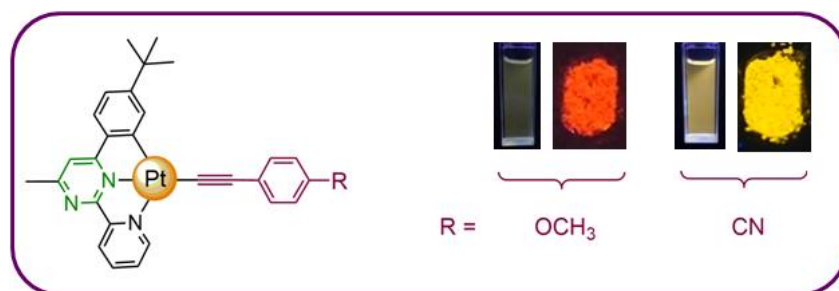
N^NC platinum (II) complexes based on phenyl- pyridin-2-ylpyrimidine ligands : synthesis, electrochemical and photophysical properties

Mariia Hruzd,^a Sébastien Gauthier,^{a,*} Julien Boixel,^a Samia Kahlal,^a Nicolas le Poul,^b Jean-Yves Saillard,^a Sylvain Achelle,^{a,*} and Françoise Robin-le Guen,^{a,*}

^a Univ. Rennes, CNRS, ISCR (Institut des Sciences Chimiques de Rennes) - UMR 6226, F-35000 Rennes, France. E-mail: sebastien.gauthier@univ-rennes1.fr, sylvain.achelle@univ-rennes1.fr, francoise.le-guen@univ-rennes1.fr.

^b Laboratoire de Chimie, Électrochimie Moléculaires et Chimie Analytique, UMR CNRS 6521, Université de Bretagne Occidentale, UFR Sciences et Techniques, 6 avenue Victor Le Gorgeu – CS 93837, F-29238 Brest Cedex 3, France.

TOC



Abstract

A series of luminescent chloro- and alkyne-platinum(II) complexes containing various tridentate cyclometalated ligands derived from phenyl-pyridin-2-ylpyrimidine and alkyne ligands has been successfully synthesized and characterized. Their electrochemical, electronic absorption and luminescence properties have been experimentally investigated and supported by (Time-Dependent) Density Functional Theory ((TD)-DFT) calculations. Electrochemical studies show the presence of a ligand-centered reduction originating from the cyclometalating N[^]N[^]C ligands, as well as a major ligand-centered oxidation process (N[^]N[^]C or alkyne) with minor contributions of the metal. Most of the complexes exhibits yellow-to-red luminescence at room-temperature in diluted solutions, in frozen matrices and in the solid state. Electron-withdrawing groups on the alkyne-ligand induce a red shift of the emission band with increased quantum yield in solution. The emission is also sensitive to the position of the pyridyl fragment on the pyrimidine core: complexes with electron-poorer 4-pyridin-2-ylpyrimidine ligands exhibit red-shifted emission and decreased quantum yield compared to their 2-pyridin-4yl analogues. In solid state, chloro-platinum complexes without *t*Bu bulky group exhibit red-shifted excimer emission.

Keywords : Platinum (II) complexes ; Pyrimidine ; N^NC Ligand ; Phosphorescence ; Alkynyl complexes

Introduction

During the past two decades, with the development of second generation organic light emitting diodes (OLEDs) based on phosphorescent emitters, there has been a great interest in the design of luminescent transition metal complexes.¹ Indeed, 75% of electrically generated excitons are triplets and for classical fluorescent materials, the external quantum efficiency is therefore limited to 25%.² In this context, cyclometallated iridium (III) complexes have been extensively developed.³ Platinum (II) complexes, even if less explored, also exhibit particularly interesting emission properties.⁴ They display tunable emitting color over the entire visible spectrum and beyond depending of the structure of the ligands,⁵ high photoluminescence quantum yield and long live excited state with triplet nature.⁴ For luminescent cyclometallated Pt (II) complexes, tridentate ligands based on azaheterocycles can be used.⁶ Complexes with N^CN ligand are generally highly luminescent.^{4,7} With N^NC ligands, Pt(II) complexes can be less emissive due to a large structural distortion of the emitting triplet state,⁸ but appropriate structural modifications of the tridentate ligand and choice of ancillary ligand permit to overcome this problem and high emission quantum yield can be obtained especially in solid state.^{4,6} In particular the extension of π -conjugation of cyclometalated ligand⁹ and the use of phenylacetylide bearing electron-withdrawing group as ancillary ligand¹⁰ tend to significantly enhance the emission quantum yield.

Pyrimidine is a six membered heterocycle bearing two nitrogen atoms in position 1 and 3. This aza-heterocycle exhibits a more pronounced π -deficient character than pyridine. This fragment has been extensively used as electron-withdrawing group for organic push-pull chromophores for luminescent and nonlinear optical properties.¹¹ The pyrimidine core can be

easily substituted in position 2 and 4 by (hetero)aromatic groups to form tridentate ligands.¹² Some phosphorescent Pt(II) complexes bearing bidentate¹³ or tridentate¹⁴ pyrimidine ligands have been described in the literature.

In this work, we designed a series of Pt(II) complexes based on phenyl-pyridin-2-ylpyrimidine ligands (Chart 1). The effects of the position of substituents on the pyrimidine core and the nature of the ancillary ligands on the photochemical and electrochemical properties of complexes were thoroughly investigated experimentally and theoretically.

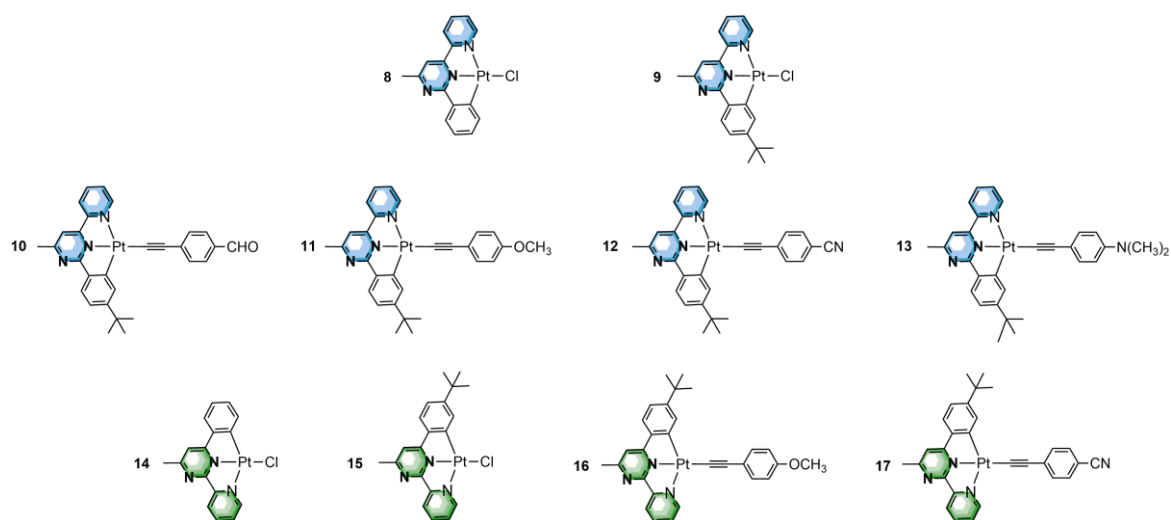
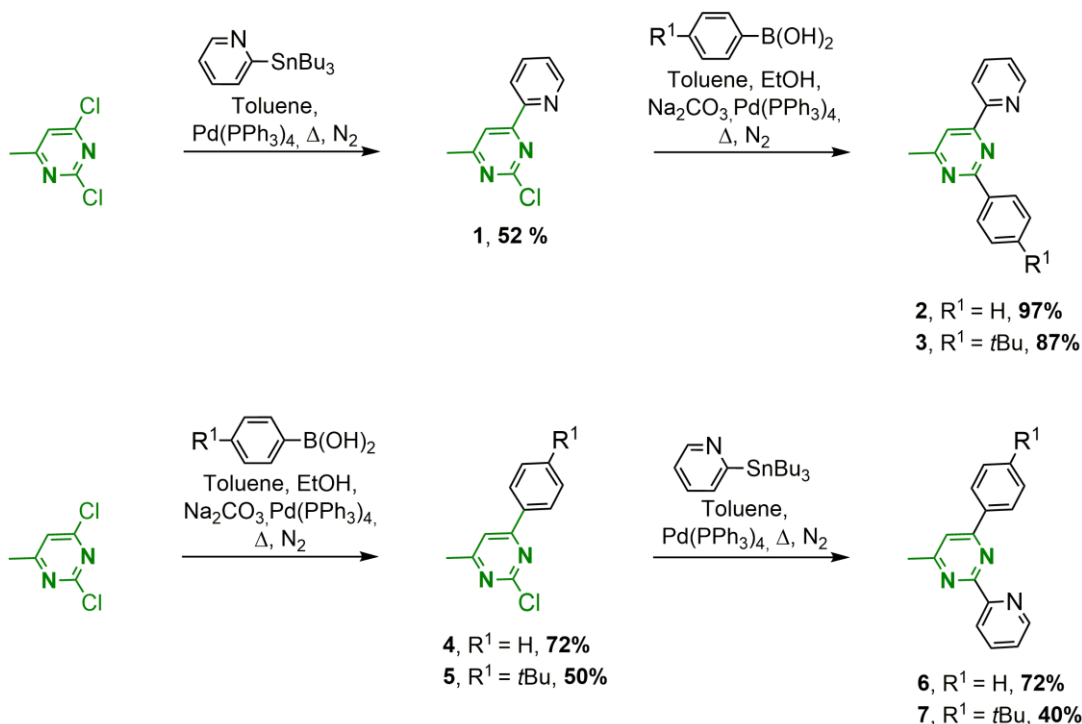


Chart 1. Structural formulas of N^NC cyclometalated Platinum(II) complexes **8-17**.

Results and discussion

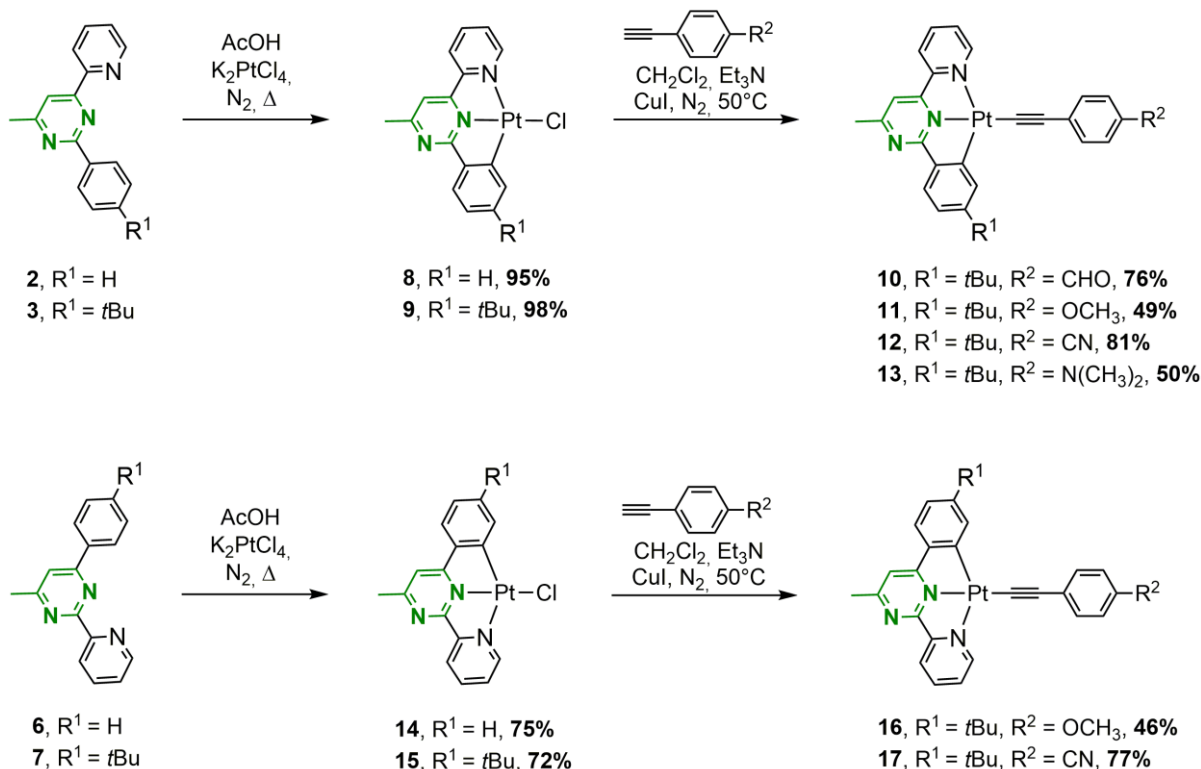
Synthesis and characterization

The synthesis of the complexes requires the cyclometalating tridentate ligands **2**, **3**, **6** and **7** whose preparation was accomplished in a two-step synthesis as shown in Scheme 1. In a first step, the 2-chloro-4-methyl-6-(pyridin-2-yl)pyrimidine **1** was produced by palladium-catalyzed Stille cross-coupling reaction of 2,4-dichloro-6-methylpyrimidine with 2-(tributylstannyl)pyridine in the presence of Pd(PPh₃)₄ under reflux of toluene in moderate yield.¹⁵ In the second step, the mono-halogen derivative **1** was converted into the corresponding ligands **2** and **3** under Suzuki-Miyaura cross-coupling reaction in presence of the appropriate boronic acids in good yields.¹⁶ The ligands **6** and **7** were prepared by reactions similar to those described for **2** and **3**, but using the Suzuki-Miyaura cross-coupling reaction as initial step, followed by a Stille cross-coupling reaction. As already observed, the coupling reactions using one equivalent of stannyl or boronic acid derivatives with 2,4-dichloro-6-methylpyrimidine exhibit good selectivity with only the mono-coupling product in position 4 of the pyrimidine being obtained.¹⁷



Scheme 1. Synthesis of the N^N^C ligands **2**, **3**, **6** and **7**.

The N^N^C cyclometalated chloro-platinum(II) complexes precursors **8**, **9**, **14**, and **15** were obtained in a good yield after a 3-day reaction between the corresponding ligands and potassium tetrachloroplatinate (K₂PtCl₄) in a refluxed solution of glacial acetic acid (Scheme 2).¹⁸ The chloro-platinum(II) **9** and **15** with *t*Bu group were selected as precursors for the preparation of σ-bonded platinum(II) acetylide. This kind of functionalization with a *t*Bu group usually provides complexes that are more soluble in organic solvents and reduces aggregation, thus facilitating the purification and chemical characterization of the compounds. Thereby, N^N^C cyclometalated alkynyl-platinum(II) complexes **10-13**, **16**, and **17** were prepared under conventional cross-coupling condition by reaction of chloro-platinum(II) precursors **9** and **15** with the corresponding organic alkynes in the presence of a catalytic amount of copper(I) iodide and triethylamine at 50°C.¹⁹ All complexes are air-stable and soluble in CH₂Cl₂, CHCl₃, THF, and toluene, except the chloro-platinum(II) precursors **8**, **9**, **14**, and **15** which display low solubility in common organic solvents.



Scheme 2. Synthesis of N^N^C Cyclometalated Platinum(II) Complexes **8-17**.

The new ligands were characterized by NMR (¹H and ¹³C) and high resolution mass spectroscopy (HRMS). Due to their low solubility, chloro-platinum complexes **8**, **9**, and **14** have only been characterized by HRMS and elemental analysis. Alkynyl-platinum complexes **10-13**, **16**, and **17** were analyzed by ¹H NMR, IR and HRMS. The characterization data were found to be in complete agreement with the proposed structures. The $\nu_{C\equiv C}$ signature band of the metal-bonded alkynyl group, in the 2105-2085 cm⁻¹ range, is observed in the IR spectra of the complexes **10-13**, **16**, and **17**. The $\nu_{C\equiv N}$ (around 2220 cm⁻¹), $\nu_{C=O}$ (around 1680 cm⁻¹) and ν_{C-O} (around 1030 cm⁻¹) bands are characteristic of the nitrile, aldehyde and methoxy functions, respectively.

Electrochemical properties

The redox properties of the N^NC cyclometalated platinum complexes were investigated by cyclic voltammetry (CV) at a Pt working electrode in CH₂Cl₂/NBu₄PF₆ 0.1 M. The electrochemical data are gathered in Table 1. All complexes display common CV features, including one reversible system in reduction at *ca.* $E_{1/2}(1) = -1.6$ V vs. Fc⁺⁰, and one quasi-reversible or irreversible anodic peak at *ca.* $E_{pa}(2) = 0.5$ V in oxidation (Figure 1). The values of the redox potentials are fully dependent on the nature of the ligands, for both reduction and oxidation processes. The chloro-platinum complexes **8**, **9**, **14**, **15** were investigated first since they offer the possibility to rationalize the influence of the substituents on the pyrimidine moiety only on the electrochemical properties. As shown in Table 1, Figures 1A and S21, complexes **14** and **15** display $E_{1/2}(1)$ values which are 150-170 mV more negative than those found for complexes **8** and **9**. This clearly suggests that the reduction process is **more** impacted by the position of the pyridyl group (2 or 4) on the pyrimidine than by the nature of the substituent (*t*Bu or H) on the phenyl ring. This result is in agreement with previous studies on analogous chloro-platinum complexes bearing various nitrogen and substituted-phenyl.^{13b,14b} In oxidation, voltammetric studies of complexes **8**, **9**, **14** and **15** show that the process is dependent on the *t*Bu or H substituents, since complexes **8** and **14** display lower $E_{pa}(2)$ values than **9** and **15** (120-160 mV difference, see Table 1). This result is consistent with DFT calculations which give computed HOMO energies at -6.38, -6.32, -6.49 and -6.37 eV for **8**, **9**, **14**, and **15**, respectively. The computed ionization energies of the four complexes (Table 1) confirm this tendency. Additionally, cyclic voltammetry shows that the oxidation is partially reversible at $\nu = 0.1$ V s⁻¹ for **8** and **14** (Figure 1A), whereas it is totally irreversible for **9** and **15** under strictly identical conditions. Such difference of reversibility in oxidation can be explained based on previous studies on cyclometalated platinum complexes.^{14b} The oxidation process is partially localized on the metal center with a major

N[^]N[^]C cyclometalated-ligand contribution (see DFT calculations, *vide supra*) and generates a transient Pt(III) species, which may be stabilized by the solvent. The lifetime of the oxidized complex is thus close to the timescale of the CV experiment, yielding partially-reversible or irreversible anodic peaks.

Voltammetric studies of alkynyl-platinum complexes bearing various substituted phenylacetylide ligands were also performed. As shown in Table 1, $E_{pa}(2)$ increases slightly with the electron-withdrawing properties of the substituent (OCH₃ vs. CN or CHO) for the **10-12** and **16-17** series. This suggests that the oxidation occurring on alkynyl-ligand with of a small contribution of the metal. However, this trend should be taken with caution given the broadness of the irreversible peaks. Furthermore, the R²-dependent orientation of the phenylacetylide ring with respect to the Pt coordination plane (see DFT calculations, *vide supra*) may induce deviation from the expected linear variation $E_{pa}(2)$ with electron-withdrawing or donor properties in this series. Finally, comparison between complexes **11** and **16**, or **12** and **17** confirms that the location of the pyridyl group in position 2 on the pyrimidine induces a negative shift (*vs.* 4-positioned) of the reduction potential $E_{1/2}(1)$ by 150-160 mV (Figure S21), as found for chloro-Pt complexes, without significantly affecting the oxidation potential. This effect is can be clearly seen in Figure 1B.

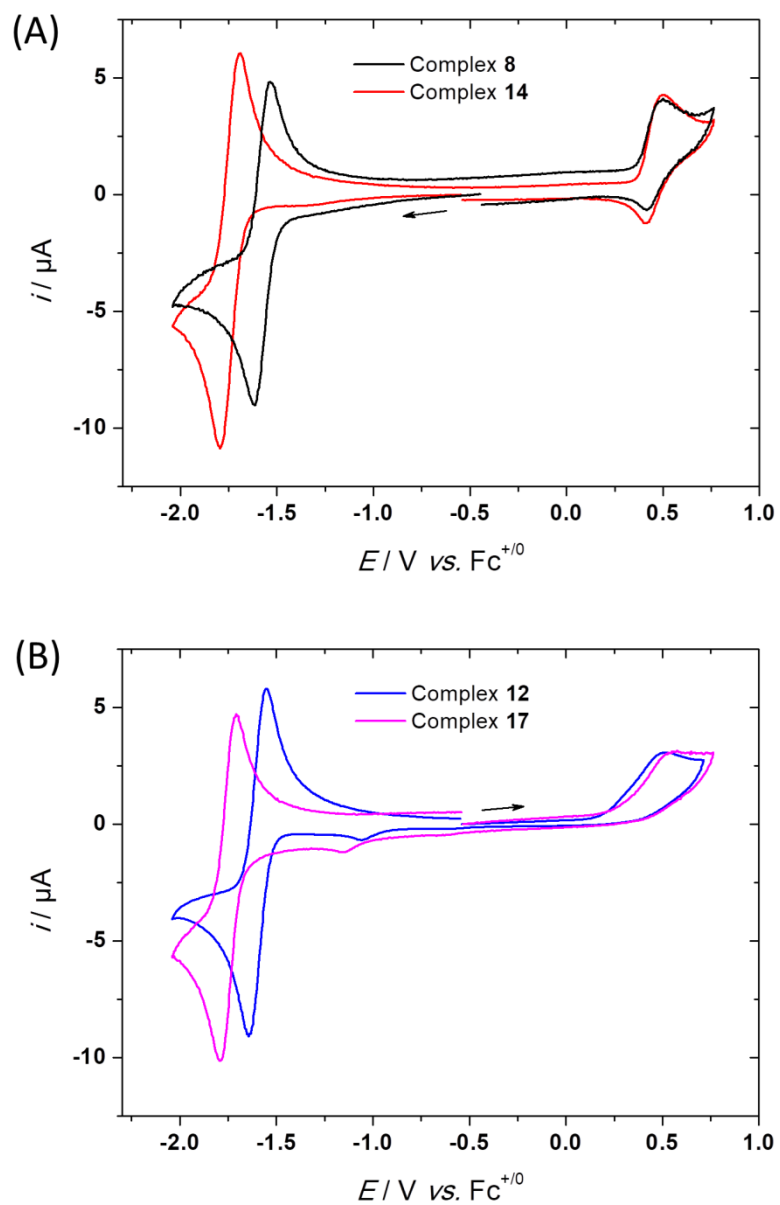


Figure 1. CVs at a Pt electrode of complexes **8** and **14** (A) (negative scanning), complexes **12** and **17** (B) (positive scanning) in $\text{CH}_2\text{Cl}_2/\text{NBu}_4\text{PF}_6$ 0.1 M ($\nu = 0.1 \text{ V s}^{-1}$, $C = 0.5 \text{ mM}$). The arrow indicates the initial sweeping direction.

Table 1. Top: Electrochemical data ($E^0(1)$ and $E_{pa}(2)$) for complexes **8-17** (0.5 mM) at a Pt working electrode in $\text{CH}_2\text{Cl}_2/\text{NBu}_4\text{PF}_6$ 0.1 M ($E / \text{V vs. Fc}^{+/0}$, $\nu = 0.1 \text{ V s}^{-1}$). Bottom: DFT-computed electron affinities (EA), ionization energies (IE) in eV HOMO-LUMO gap (eV) and Dipole moment (D) in CH_2Cl_2 .

	8	9	10	11	12	13	14	15	16	17
$E_{1/2}(\mathbf{1})$	-1.57	-1.61	-1.60	-1.61	-1.59	-1.61	-1.74	-1.76	-1.76	-1.75
$E_{pa}(\mathbf{2})$	0.49	0.61	0.56	0.46	0.51	0.02 ^a	0.50	0.66	0.47	0.55
EA	3.07	3.05	3.07	3.01	3.06	2.98	2.88	2.85	2.83	2.89
IE	6.15	6.02	5.76	5.22	5.80	4.78	6.17	6.12	5.22	5.80
HOMO-LUMO gap	3.67	3.63	3.92	3.89	3.35	2.89	3.38	2.47	3.09	3.58
Dipole moment	14.34	13.43	11.68	10.79	17.34	12.91	18.94	10.24	9.39	17.07

^a Irreversible anodic peak whose low potential value can be ascribed to the high contribution of the dimethylamino moiety to the HOMO (see Fig. S7).

Photophysical properties

The photophysical properties of the synthesized chloro- and alkynyl-platinum(II) complexes have been investigated in solution using UV-visible absorption and luminescence spectroscopies. The steady-state absorption and luminescence spectra of complexes **10-13**, **16** and **17**, are presented in Figures 2, 3, and 4, respectively, and the related data are summarized in Table 2.

Chloro-platinum complexes **8**, **9**, **14** and **15**, show characteristic UV-visible absorption features with a set of intense absorption bands in the UV region, from 250 to 370 nm, assigned to intra-ligand (IL) $^1\pi-\pi^*$ transitions on the functionalized cyclometalated ($\text{N}^{\wedge}\text{N}^{\wedge}\text{C}$) ligands and moderately intense absorption bands from 385 to 420 nm, attributed to an admixture of intra-ligand $^1\text{ILCT } \pi_{\text{Ph}}(\text{N}^{\wedge}\text{N}^{\wedge}\text{C}) \rightarrow \pi^*_{\text{bpy}}(\text{N}^{\wedge}\text{N}^{\wedge}\text{C})$ and metal-to-ligand $^1\text{MLCT } d(\text{Pt}) \rightarrow \pi^*(\text{N}^{\wedge}\text{N}^{\wedge}\text{C})$ charge transfer. The two 4-pyridyl complexes **8** and **9** exhibit additional

lower-lying absorption bands tailing up to 550 nm, in line with their smaller computed (see below) and voltammetric (Table 1) HOMO-LUMO gaps. For both 2-pyridyl and 4-pyridyl chloro-platinum series, the *t*Bu group on the phenyl part of the cyclometalated ligand has a minor influence on the absorption features.

The alkynyl-platinum complexes (**10-13**, **16** and **17**) show broad low-energy absorption bands of large ligand-to-ligand charge transfer nature (${}^1\text{LL}'\text{CT } \pi(\text{phenylacetylide}) \rightarrow \pi^*(\text{N}^{\wedge}\text{N}^{\wedge}\text{C})$, see below), which strongly depend on the nature of the alkynyl ligand. Complexes **16** and **17**, belonging to the 2-pyridyl series, show different absorption spectra ascribed to the opposed electronic characters of the alkynyl ligands; *i.e.*: electron-withdrawing (EWG: *p*-benzonitrile, for **16**) and electron-donating (EDG: *p*-anisole, for **17**) groups. Intense absorption bands, both in the UV (centered at 311 nm) and in the visible (from 375 to 500 nm) regions exhibiting an absorptivity twice that of the complex **16** bands, are observed for complex **17**.

However, complex **16** exhibits lower-lying transitions up to 575 nm attributed to its destabilized HOMO (see Figure S36), induced by the electron-donating character of its alkynyl ligand. Similar influences of the terminal function of the alkynyl ligand are observed for the 4-pyridyl series: Complex **11**, bearing the *p*-anisole group, shows extended absorption tailing to 600 nm, while complexes **10** and **12**, with *p*-benzaldehyde and *p*-benzonitrile respectively, display CT bands from 475 to 550 nm. When comparing the two 2- and 4-pyridyl series with the same alkynyl ligand (**12** vs **17** and **11** vs **16**), the 4-pyridyl series exhibits bathochromic shifts of the charge-transfer transitions ($\Delta\lambda \approx 20$ nm) in accordance with the less negative reduction potential $E_{1/2}(1)$ recorded for complexes **11** and **12** compared to **16** and **17** (Figure 1B and Table 1).

With the exception of complex **13**, all the new platinum complexes exhibit luminescence at room-temperature in diluted solutions, in frozen matrices and in the solid

state. Additional non-radiative deactivation pathway through photo-induced electron transfer can explain the luminescent-silent character of **13**.²⁰ As far as the room-temperature luminescence is concerned, chloro-platinum complexes **14** and **15** (2-pyridyl series) display structured emission profile ($\lambda_{\text{max}} = 580$ and 585 nm, respectively) with vibrational spacing of about 1100 cm^{-1} , substantiating a ligand-centered character of the emissive states. Complexes **8** and **9** (4-pyridyl series) show broad emission bands centered at 608 nm due to a charge transfer emissive state. Similarly to the observation made for their absorption features, the *t*Bu groups do not play a significant role in the luminescence energy at room-temperature. Complexes **8** and **9** exhibit bi-exponential decays as previously observed with other platinum complexes excited states.²¹ The photoluminescence quantum yields (PLQY) are about one percent for the 4-pyridyl chloro-platinum complexes **8**, **9** and of about the double for the 2-pyridyl analogues **14**, **15**. One can notice that these PLQY (1 to 2 %) are in accordance with those reported for related chloro(N^NC)-platinum complexes.²²

When comparing the alkynyl-complexes of the 2-pyridyl series, **16** and **17**, the OMe electron-donating group (in **16**) red-shifts the λ_{max} of $\Delta\lambda = 762\text{ cm}^{-1}$ and drastically diminishes the emission intensity by a factor 5.5. This observation can be ascribed to additional nonradiative deactivation pathways through population of low-lying states (³ILCT and ³LLCT). Similarly, **11** bearing the *p*-anisole alkyne ligand in the 4-pyridyl series, exhibits red-shifted emission ($\Delta\lambda_{\text{max}} = 940\text{ cm}^{-1}$) and a diminished PLQY (2.5 folds) with regards to the benzonitrile analogue **12**. Replacing the benzonitrile group by the benzaldehyde (**10**) gives similar PLQY and luminescence decay times, revealing comparable photophysical behaviors. Interestingly, the isomers **17** and **12** carrying the benzonitrile ligand in the 2- and 4-pyridyl series, respectively, display large differences in their emission features. The PLQY ratio is about 2.6 for **17/12** and the λ_{max} shift reaches 975 cm^{-1} , from **17** to **10**. An even more

pronounced red-shift of 46 nm is observed between **16** and **11**, while they display similar low PLQY.

Figure S22 shows the luminescence spectra of complexes **8-12** and complexes **14-17** recorded in EPA mixture at 77 K. All the latter complexes display highly structured emission profile with vibrational spacing from around 1280 to 1380 cm^{-1} , 100 to 200 cm^{-1} higher than those reported for related 6-phenyl-2,2'-bipyridine platinum(II) complexes.²³ The 0-0 emission bands of the chloro-platinum complexes are distributed according the electron richness of the ligand, starting with the complexes from the 2-pyridyl series (**14** < **15**) then the two of the 4-pyridyl series (**8** < **9**). One can notice that unlike room-temperature emission, the inductive effect of the *t*Bu groups induces a slight bathochromic shift on the emission energy. Within the alkynyl-platinum series, the nature of the cyclometalated ligand impacts the emissive energy level with lower λ_{max} for the 2-pyridyl series, complexes **16** and **17**, than for the 4-pyridyl analogues complexes **11** and **12**. Also, the electron-richness of the aryl alkyne ligand induces drastic shifts of the emission energy, *i.e.*; within the 2-pyridyl series **16** and **17** that bear benzonitrile and anisole groups respectively show a $\Delta\lambda_{\text{max}}$ of 41 nm (from $\lambda_{\text{max}} = 526$ to 567 nm), and for the 4-pyridyl series **10/12** (benzonitrile group: $\lambda_{\text{max}} = 548/545$ nm) versus **11** (anisole group $\lambda_{\text{max}} = 589$ nm) a $\Delta\lambda_{\text{max}}$ of 43 nm is observed. Regarding the emission lifetimes of the chloro-platinum complexes, the 2-pyridyl series shows luminescence decays similar to that of 6-phenyl-2,2'-bipyridine analogues with about 7 – 8 μs , while the 4-pyridyl complexes exhibit twice the decay time with around 15 – 18 μs . Similar trends of longer emission life-time are observed in the alkynyl platinum complexes series with 40 % increased decays for the 4-pyridyl complexes.

The solid-state luminescence of the chloro-platinum complexes **8** and **14** displays broad emission bands at 687 and 711 nm, respectively. These structureless low-energy emission originate probably from excimer formation more than from metal-metal-to-ligand

charge transfer MMLCT emission²⁴ as shown by the concentration dependent experiments demonstrating the respect of the Beer Lambert law (Figures S27-S30). The other complexes do not exhibit such excimer emission due to the hindering *t*Bu group. Complexes **9-12** and **15-17** display structured solid-state emission with comparable 0-0 emission energy than that observed in frozen matrices (Figure 5). Complexes **11**, **15** and **16** present both structured and broad excimer emission bands even though they bear a *t*Bu group.

Table 2. Absorption and emission data in solution for platinum complexes **8-17**.

298 K			77 K
$\lambda_{\text{abs}}^{\text{a}}$ / nm (ϵ / mM ⁻¹ cm ⁻¹)	$\lambda_{\text{em}}^{\text{b}}$ / nm [τ^{c} /ns]	Φ^{d}	$\lambda_{\text{em}}^{\text{e}}$ / nm [τ^{e} μ s]
8 276 (21.8), 328 (7.0), 385 (3.6), 458 (2.6)	608 [17(86%), 301(14%)]	0.012	531 [17.9], 570, 617
9 279 (26.1), 294sh (22.4), 339 (7.4), 387 (4.5), 458 (2.7)	608 [21(90%), 167(10%)]	0.014	544 [15.0], 585, 639
10 285 (24.3), 337 (21.2), 382sh (9.4), 464 (4.7)	628 [70]	0.021	548 [8.7], 592, 643sh
11 282 (37.6), 345 (7.4), 388 (7.2), 483 (4.8)	655 [/]	0.009	589 [12.5], 637
12 281 (59.5), 380 (6.2), 462 (3.6)	617 [60]	0.023	546 [9.0], 587, 643sh
13 293 (32.0), 394 (5.6), 494 (3.5)	/	/	/
14 266 (20.4), 291 (17.9), 321 (11.1), 390 (5.3), 429sh (2.9)	544, 580 [47]	0.021	514 [8.0], 553, 598
15 266 (16.4), 299 (15.3), 328sh (9.9), 386 (4.2), 429sh (2.0)	551, 585 [47]	0.018	526 [7.2], 564, 605
16 270 (32.3), 294sh (25.2), 311sh (18.9), 332sh (11.7), 394 (7.4), 464 (4.0)	609 [/]	0.010	567 [9.3(74%), 4.2(26%)], 610, 652sh
17 265 (30.8), 280 (33.6), 311 (51.3), 391 (13.7), 422sh (10.7), 449sh (7.0)	582 [160]	0.055	525 [6.2], 566, 613

^a Measured in CH₂Cl₂ solution at 298 K ($C \approx 10^{-5}$ M). ^b In degassed CH₂Cl₂ solution at 298 K ($C \approx 10^{-5}$ M, $\lambda_{\text{ex}} = 420$ nm). ^c $\lambda_{\text{ex}} = 375$ nm. ^d With Ru(bpy)₃Cl₂ as reference. ^e in EPA at 77K ($\lambda_{\text{ex}} = 420$ nm). sh = shoulder

Table 3. Emission data in the solid state (powder) at 298 K for platinum complexes **8-12** and complexes **14-17**.

	$\lambda_{em}^a / \text{nm} [\tau^b/\text{ns}]$
8	711 [/]
9	547, 584, 624 [169(74%), 848(26%)], 682sh
10	612 [370(80%), 59(20%)], 644
11	601 [61(18%), 208(82%)], 639, 730br
12	543, 583, 605 [83(76%), 565(24%)], 661sh
14	687 [105(25%), 254(75%)]
15	517, 559, 605 [98(75%), 455(25%)], 700br
16	627 [20(9%), 103(31%), 468(60%)]
17	552, 589 [61(43%), 338(57%)], 636

^a $\lambda_{ex} = 420 \text{ nm}$. ^b $\lambda_{ex} = 375 \text{ nm}$. sh = shoulder, br = broad.

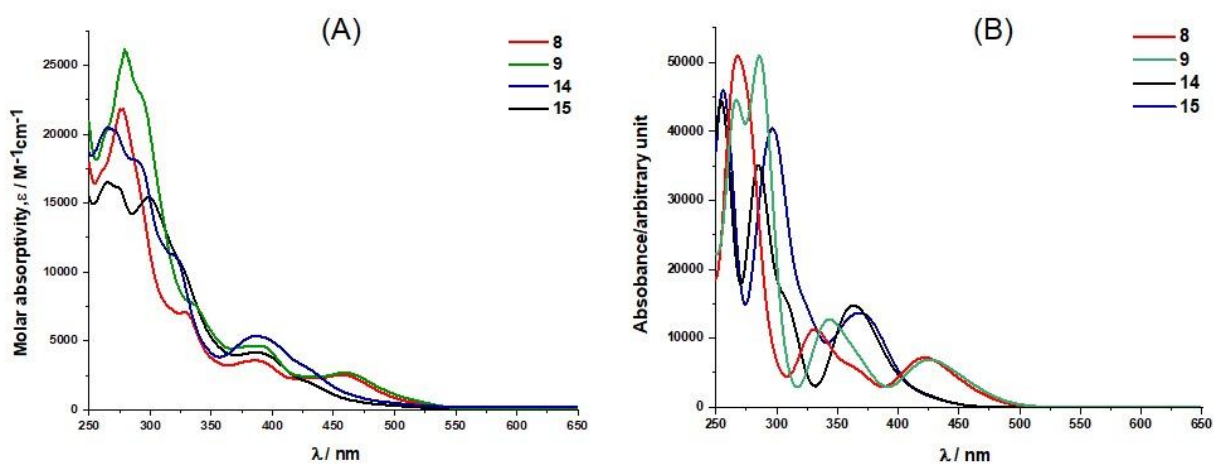


Figure 2. (A): Absorption spectra in dichloromethane of chloro-platinum complexes (**8**, **9**, **14** and **15**) ($C \approx 10^{-5} \text{ M}$); (B): TD-DFT-simulated UV-vis absorption spectra of chloro-platinum complexes (**8**, **9**, **14** and **15**).

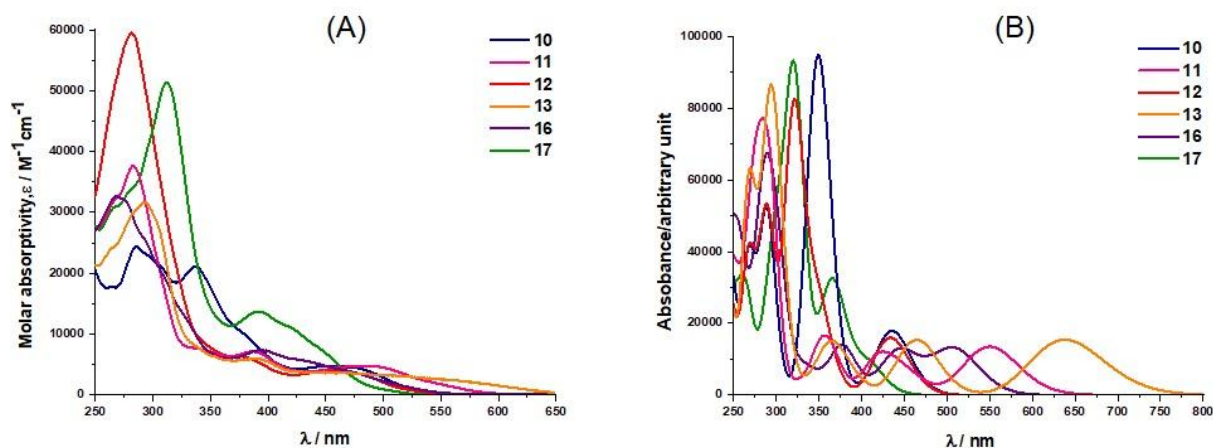


Figure 3. (A): Absorption spectra in dichloromethane of alkyne-platinum complexes (**10-13**, **16** and **17**) ($C \approx 10^{-5}$ M); (B): TD-DFT-simulated UV-vis absorption spectra of alkyne-platinum complexes (**10-13**, **16** and **17**).

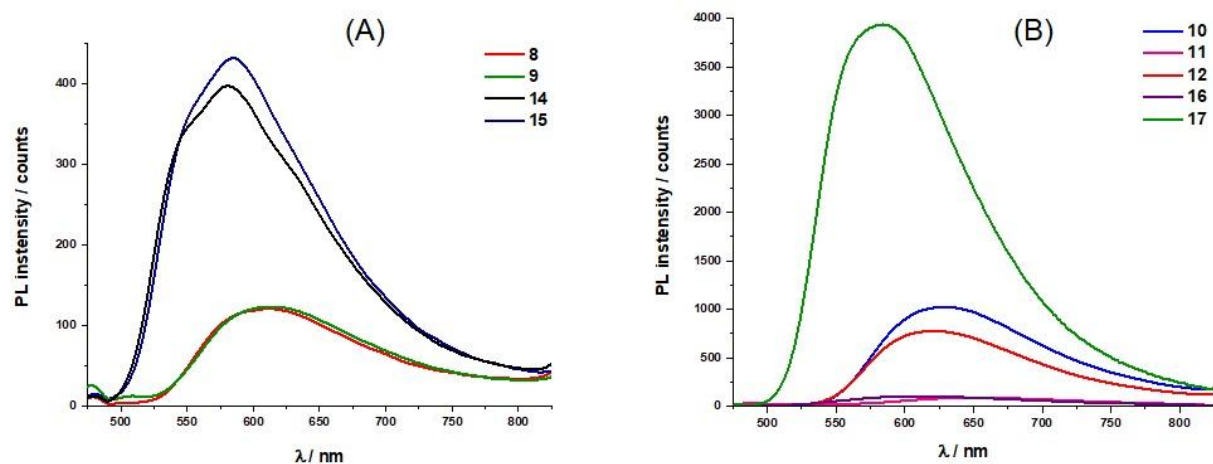


Figure 4. Emission spectra in degassed dichloromethane at 298 K of chloro-platinum complexes **8**, **9**, **14** and **15** (A) and alkyne-platinum complexes **10-12**, **16** and **17** (B) ($C \approx 10^{-5}$ M, $\lambda_{\text{ex}} = 420$ nm).

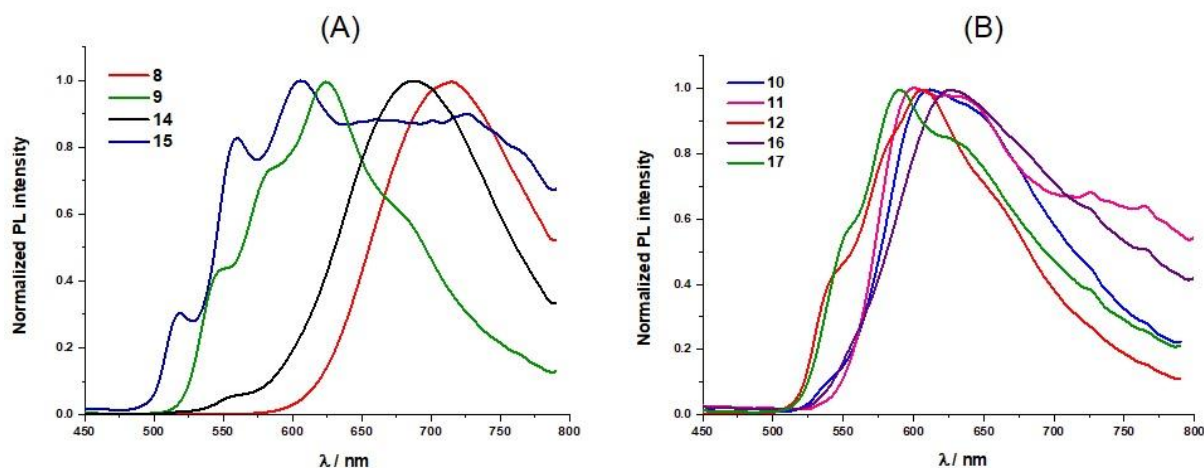


Figure 5. Emission spectra in the solid state (powder) at 298 K of chloro-platinum complexes **8**, **9**, **14** and **15** (A) and alkynyl-platinum complexes **10-12**, **16** and **17** (B) ($\lambda_{\text{ex}} = 420$ nm).

Computational studies

Density functional theory (DFT) calculations at the PBE0/LANL2DZ level of theory were performed to optimize the geometries of complexes **8-17**. Solvent (CH_2Cl_2) effect corrections were included (see Computational Details). The optimized geometries, characterized as true minima by vibrational frequency calculations, are shown in Figure 6. Selected computed data are provided in Table 1 and S4. The ten complexes exhibit comparable optimized geometries, with rather similar metrical data. One can note that the chloro-platinum complexes **8**, **9**, **14** and **15** have slightly stronger Pt-N and Pt-C bonds than their phenylacetylide relatives. Within the phenylacetylide series, the major structural differences lie in the orientation of the phenylacetylide ring with respect to the Pt coordination plane. When this ring bears an electron-attracting group (CN or CHO), it is perpendicular to

the rest of the molecule (complexes **10**, **12** and **17**), whereas in all the other compounds the molecule is close to ideal planarity. Obviously, the 16-electron metal center is maximizing its back-donation to the phenylacetylide ligand by using its π in-plane lone pair. This stronger conjugative effect is in line with the lowest C \equiv C Wiberg index values for **10**, **12** and **17**. Consistently, the three complexes have the largest dipole moments of the series (Table 1). The Kohn-Sham MO diagrams of complexes **8-17** are provided in Figures S35 and S36. Their frontier orbitals are plotted in Figures S37 and S38. They all exhibit a similar LUMO with a large (93-95%) localization on the two conjugated heterocycles, which can be identified as the π^* LUMO of the free N $^{\wedge}$ N $^{\wedge}$ C ligand. The HOMOs of the chloro-platinum complexes **8**, **9**, **14** and **15** have their major contribution from a π -type orbital of the N $^{\wedge}$ N $^{\wedge}$ C C₆ ring, with non-negligible (33-36%) metal 5d(π) participation and no Cl participation. On the other hand, the alkynyl-platinum complexes **10-13**, **16** and **17** have their HOMOs mainly (74-88%) localized on the phenylacetylide chain.

The electron affinities (*EI*) of complexes **8-17**, computed as the energy differences between the complexes and their anions (both in their equilibrium geometries), are given in Table 1. They correlate reasonably well with the CV-recorded $E_{1/2}(1)$ values and confirm the major influence of the position of the pyridyl group (Figure S33, left). A very similar correlation can be found between $E_{1/2}(1)$ and the LUMO energies (Figure S34), indicating that no significant structural or electronic rearrangement occurs upon reduction. The correlation between the recorded $E_{pa}(2)$ potentials and the ionization energies (IE) calculated as the energy differences between the complexes and their anions (both in their equilibrium geometry) is more approximate (Table 1 and Figure S33, right). This can be attributed to the non-reversible nature of $E_{pa}(2)$ and/or the perpendicular or parallel orientation of the phenylacetylide ring with respect to the Pt coordination plane according to the R² substituent.

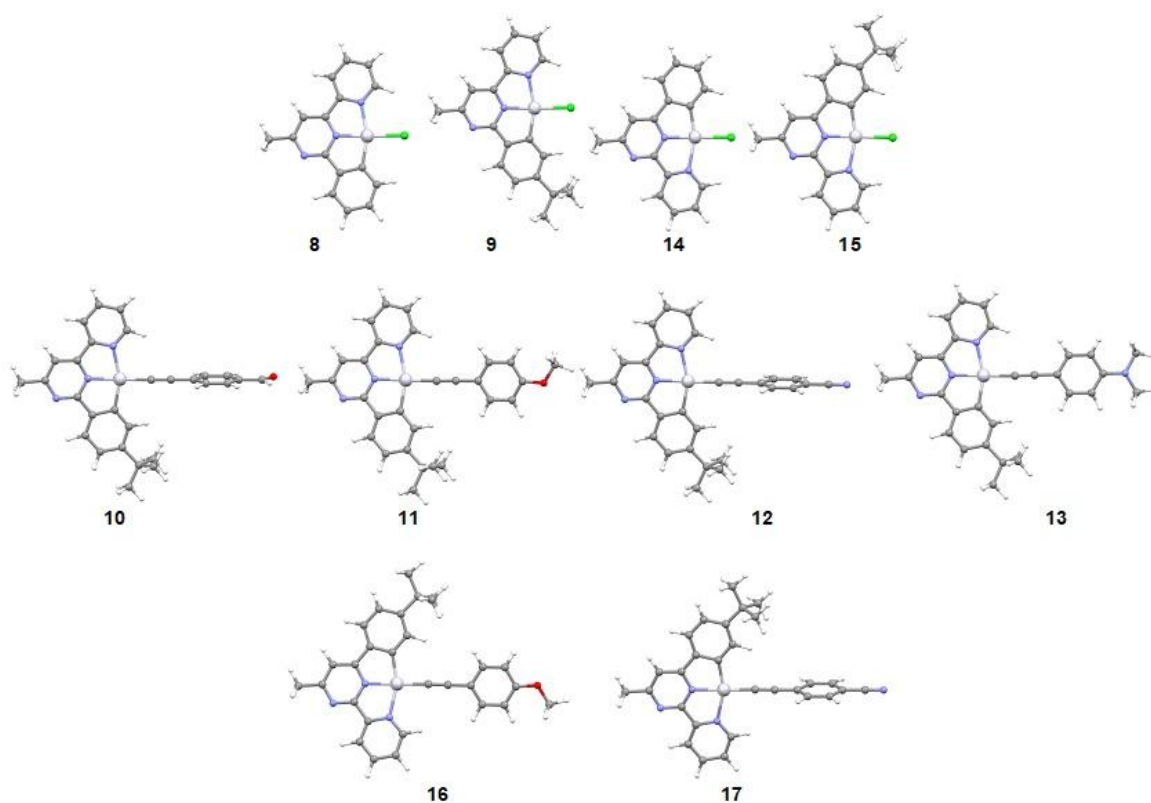


Figure 6: DFT-optimized geometries of complexes **8-17**.

The TD-DFT-simulated UV-vis spectra of complexes **8-17** are shown on Figures 2 (B) and 3 (B). They are in quite good agreement with their experimental counterparts (Figures 2 (A) and Figure 3 (A)). The transitions associated with the band of lower energy can be associated with HOMO→LUMO transitions and therefore reflect the HOMO-LUMO gaps. It follows that, in the case of chloro-platinum complexes **8, 9, 14** and **15**, it is of major intraligand character (see their plot in Figure S37). The other major bands of these chloride derivatives can also be described as intraligand $\pi\rightarrow\pi^*$ transition with some (modest) admixture of MLCT. The situation is different for alkynyl-platinum complexes **10-13, 16** and **17** for which the transition of lowest energy (HOMO→LUMO, see Figure S31) is associated with a $\pi(\text{phenylacetylide})\rightarrow\pi^*(\text{N}^-\text{N}^+\text{C})$ charge transfer (LL'CT). The other computed transitions are of the same ILCT nature as that of their chloride relatives.

Conclusion

In conclusion, a new class of luminescent N^NC-cyclometalated chloro- and alkynyl-platinum(II) complexes has been synthesized and characterized. The electrochemical and photophysical properties of these complexes have been carefully studied with the help of (TD-)DFT calculations and except **for** complex **13**, all exhibit yellow-to-red emission in solution and solid state. The following structure-property relationships can be highlighted:

- For chloro-platinum complexes, the absence of *t*Bu substituent on the phenyl ring of N^NC ligand induces a lower oxidation potential ($\Delta E_{pa} = 0.12\text{-}0.16$ V), as well as a red-shifted excimer emission in solid state. In solution, the presence of *t*Bu has no significant effect on the photophysical properties.
- The presence of alkynyl ligand shifts the oxidation potential of complexes. The alkynyl-platinum complexes display broad low-energy absorption bands of long-range ligand-to-ligand charge transfer nature (¹LL'CT), which strongly depend on the R² substituent of the alkynyl ligand. CN and CHO electron withdrawing substituents induce hypochromic shift of the less energetic absorption band with regards to methoxy analogues. Similarly, electron-withdrawing substituents lead to blue-shifted emission with increased PLQY.
- The position of the pyridyl substituent also plays a significant role on the electrochemical and photophysical properties: complexes with electron-poorer 4-pyridin-2-ylpyrimidine ligands exhibit a more positive reduction potential than the potential found for the 2-pyridyl complexes. Moreover, they show additional lower-lying absorption bands and red-shifted emission with reduced PLQY in solution with regards to 2-pyridin-2-ylpyrimidine analogues.

Even if this new series of complexes display relatively low quantum yields, these results represent a useful study in the development of efficient phosphorescent emitters. Experiments are currently underway to modify the auxiliary and the tridentate ligands of new cyclometalated platinum(II) complexes to improve the photoluminescence properties.

Experimental part

General information

In air- and moisture-sensitive reactions, all glassware was flame-dried. All reactions were conducted under a dry nitrogen atmosphere using Schlenk techniques, but workups were used as received. The starting materials were purchased from Sigma-Aldrich, TCI or Alfa-Aesar and were used as received. The solvents and reactants were used as received except tetrahydrofuran that was distilled under a dry nitrogen atmosphere over sodium and benzophenone. Organic solutions were concentrated under reduced pressure using a rotary evaporator. Thin layer chromatography (TLC) was conducted on pre-coated aluminum sheets with 0.20 mm Merck Alugram SIL G/UV254 with fluorescent indicator UV254 and 0.25 mm Merck silica gel (60-F254). Column chromatography was carried out using Acros silica gel 60 (particle size 63-200 μm) and Macherey Nagel Aluminum neutral oxide 40 (particle size 40-160 μm). Nuclear magnetic resonance (NMR) spectra were acquired at room temperature on a Bruker AC-300 spectrometer (^1H at 300 MHz, ^{13}C at 75 MHz,) and referenced as follows: ^1H NMR, residual CHCl_3 ($\delta = 7.26$ ppm); $^{13}\text{C}\{^1\text{H}\}$ NMR, internal CDCl_3 ($\delta = 77.16$ ppm). The chemical shifts δ are reported in parts per million relative to TMS (^1H , 0.0 ppm) and CDCl_3 (^{13}C , 77.16 ppm). The coupling constant J is given in Hz. In the ^1H NMR spectra, the following abbreviations are used to describe the peak pattern: *s* (singlet), *d* (doublet), *dd* (doublet of doublet), *t* (triplet), and *m* (multiplet). Acidic impurities in CDCl_3 were removed by treatment with anhydrous K_2CO_3 . IR spectra were recorded on a Perkin-Elmer spectrum

100 spectrometer with an ATR sampling accessory. High Resolution Mass Spectrometry (HRMS) analyses were performed at the “Centre Régional de Mesures Physiques de l'Ouest” (CRMPO, University of Rennes 1, France) using a Bruker MicroTOFQ II apparatus.

Cyclic voltammetry

The electrochemical studies were performed in a glovebox (Jacomex) ($O_2 < 1$ ppm, $H_2O < 1$ ppm) with a home-made 3-electrode cell (WE: Pt, RE: Ag wire, CE: Pt). Ferrocene was added at the end of each experiment to determine the redox potential values. The standard potential of the Fc^+/Fc couple in CH_2Cl_2/NBu_4PF_6 was measured experimentally with reference to the standard calomel electrode (SCE): $E^0(Fc^+/Fc) = 0.47$ V vs. SCE. The potential of the cell was controlled by an AUTOLAB PGSTAT 100 (Metrohm) potentiostat monitored by the NOVA[®] software (Metrohm). Dichloromethane was freshly distilled from CaH_2 and kept under Ar in the glovebox. Tetrahydrofuran (99.9%, HPLC) was stored in the glovebox and dried over molecular for 48h before use. The supporting salt NBu_4PF_6 was synthesized from NBu_4OH (Fluka) and HPF_6 (Aldrich). It was then purified, dried under vacuum for 48 hours at $100^\circ C$, and then kept under N_2 in the glovebox.

Photophysical details

UV/vis absorption spectra were recorded with a Jasco V-770 UV-Vis-NIR spectrophotometer using quartz cuvettes of 1 cm pathlength. Steady-state luminescence spectra were measured using an Edinburgh FS920 Steady State Fluorimeter combined with a FL920 Fluorescence Lifetime Spectrometer. The spectra were corrected for the wavelength dependence of the detector, and the quoted emission maxima refer to the values after correction. Luminescence quantum yields were determined using $[Ru(bpy)_3]Cl_2$ ($\Phi = 0.042$ in air-equilibrated aqueous solution)²⁵ as standard and correcting for the refractive index. Life-times measurements were

conducted with 375 nm diode laser excitation (EPL-series) plugged to a TCSPC pulsed source interface.

Computational details

DFT and TD-DFT calculations were carried out using the Gaussian16 package²⁶ employing the PBE0 functional,²⁷ together with the Def2TZVP basis set.²⁸ Solvent (dichloromethane) effects were included through the PCM approximation²⁹ in all the calculations. The optimized geometries were fully characterized as true minima by analytical frequency calculations (no imaginary values). The composition of the Kohn-Sham orbitals was calculated using the AOMix program.³⁰ The geometries obtained from DFT calculations were used to perform natural atomic charge analysis with the NBO 6.0 program.³¹ Only singlet-singlet transitions were taken into account in the TD-DFT calculations. The graphical GaussView interface³² was used for simulating UV-vis spectra.

Synthesis

2-chloro-4-methyl-6-(pyridin-2-yl) pyrimidine (1), Method A: In a Schlenk flask, aromatic 2,4-dichloro-6-methylpyrimidine (815 mg, 5 mmol, 1 equiv) was degassed by bubbling with nitrogen for 15 minutes. Toluene (60 mL) was added to the flask and stirred. Whereupon 2-(tributylstannyl)pyridine (2 g, 5.5 mmol, 1.1 equiv) was added and the mixture was stirred under nitrogen for 10 min. Pd(PPh₃)₄ (290 mg, 5 mol%, 0.05 equiv) was quickly added. The reaction was stirred under nitrogen at reflux for 24h. The mixture was allowed to cool to room temperature. The mixture was diluted with water, and the aqueous layer was extracted with EtOAc (2 × 25 mL). The separated organic phase extracts were dried over MgSO₄, filtered and the solvents were evaporated under reduced pressure. The crude product was purified by silica gel column chromatography (Petroleum ether to petroleum ether/AcOEt, 1:10, v/v) to

give compound **1** as a colorless crystalline solid in 52% yield (535 mg). NMR (δ (ppm), CDCl_3): ^1H (300 MHz): 8.71 (d, $^3J_{\text{HH}} = 3.9$ Hz, 1H), 8.47 (d, $^3J_{\text{HH}} = 7.3$ Hz, 1H), 8.19 (s, 1H), 7.87 (t, $^3J_{\text{HH}} = 7.8$ Hz, 1H), 7.46 – 7.41 (m, 1H), 2.63 (s, 3H); $^{13}\text{C}\{^1\text{H}\}$ and JMOD (75 MHz) 171.6 (C), 165.4 (C), 160.9 (C), 152.6 (C), 149.6 (CH), 137.2 (CH), 125.9 (CH), 122.2 (CH), 115.2 (CH), 24.2 (CH_3). HRMS (ESI) m/z calculated for $\text{C}_{10}\text{H}_8\text{N}_3^{35}\text{ClNa}$ [$\text{M} + \text{Na}$] $^+$: 228.0298, found: 228.0298 (0 ppm).

4-methyl-2-phenyl-6-(pyridin-2-yl)pyrimidine (2), Method B: In a Schlenk flask, **1** (1.0 g, 5 mmol, 1 equiv) and phenylboronic acid (671 mg, 5.5 mmol, 1.1 equiv) were introduced. The mixture was degassed by bubbling with nitrogen for 15 minutes. Whereupon toluene (48 mL), Na_2CO_3 saturated solution (3 ml) and EtOH (2 mL) were added. The reaction mixture was stirred under bubbling with Nitrogen into the solution for 10 min. Then $\text{Pd}(\text{PPh}_3)_4$ (290 mg, 5 mol%, 0.05 equiv) was quickly added. The reaction was stirred under nitrogen at reflux for 48h. The mixture was diluted with water, and the aqueous layer was extracted with EtOAc (2 \times 25 mL). The separated organic phase extracts were dried over MgSO_4 , filtered and the solvents were evaporated under reduced pressure. The crude product was purified by silica gel column chromatography (Petroleum ether to petroleum ether/AcOEt, 3:7, v/v) to give compound **2** as a colorless crystalline solid in 97 % yield (1.2 g). NMR (δ (ppm), CDCl_3): ^1H (300 MHz): 8.65 (d, $^3J_{\text{HH}} = 4.6$ Hz, 1H), 8.63 – 8.55 (m, 3H), 8.06 (s, 1H), 7.76 (t, $^3J_{\text{HH}} = 7.0$ Hz, 1H), 7.55 – 7.41 (m, 3H), 7.32 – 7.24 (m, 1H), 2.62 (s, 3H); $^{13}\text{C}\{^1\text{H}\}$ NMR (JMOD, 75 MHz, CDCl_3) 168.3(C), 163.8(C), 162.3 (C), 154.4 (C), 149.2 (CH), 137.9 (C), 136.8 (CH), 130.4 (CH), 128.3 (CH), 128.3 (CH), 125.0 (CH), 121.7 (CH), 114.3 (CH), 24.5 (CH_3). HRMS (ESI) m/z calculated for $\text{C}_{16}\text{H}_{14}\text{N}_3$ [$\text{M} + \text{H}$] $^+$: 248.1182, found: 248.1179 (1 ppm).

2-(4-(tert-butyl)phenyl)-4-methyl-6-(pyridin-2-yl)pyrimidine (3): The product was synthesized by *method B* according to a similar procedure employed for compound **2**, except the (4-(tert-butyl)phenyl)boronic acid (980.0 mg, 5.5 mmol, 1.1 equiv) was used in place of phenylboronic acid. The crude product was purified by silica gel column chromatography (Petroleum ether to petroleum ether/AcOEt, 10:1, v/v) to give compound **3** as a colorless crystalline solid in 87 % yield (1.1 g). NMR (δ (ppm), CDCl₃): ¹H (300 MHz): 8.69 (d, ³J_{HH} = 4.8 Hz, 1H), 8.65 (d, ³J_{HH} = 7.0 Hz, 1H), 8.51 (d, ³J_{HH} = 8.6 Hz, 2H), 8.08 (s, 1H), 7.82 (td, ³J_{HH} = 7.7, 1.8 Hz, 1H), 7.54 (d, ³J_{HH} = 8.6 Hz, 2H), 7.34 (ddd, ³J_{HH} = 7.5, 4.8, ⁴J_{HH} = 1.2 Hz, 1H), 2.65 (s, 3H), 1.39 (s, 9H); ¹³C{¹H} NMR (JMOD, 75 MHz, CDCl₃) 168.4 (C), 164.2 (C), 162.4 (C), 154.7 (C), 153.7 (C), 149.3 (CH), 137.0 (CH), 135.4 (C), 128.2 (CH), 125.4 (CH), 125.1 (CH), 121.9 (CH), 114.1 (CH), 34.9 (C), 31.3 (CH₃), 24.6 (CH₃). HRMS (ASAP) *m/z* calculated for C₂₀H₂₂N₃ [M + H]⁺: 304.1808, found: 304.1809 (0 ppm).

2-chloro-4-methyl-6-phenylpyrimidine (4): The product was synthesized by *method B* according to a similar procedure employed for compound **2**, except the 2,4-dichloro-6-methylpyrimidine (815 mg, 5 mmol, 1 equiv) was used in place of **1** and the reaction time is 24h. The crude product was purified by silica gel column chromatography (Petroleum ether to petroleum ether/AcOEt, 1:10, v/v) to give compound **4** as a white solid in 72 % yield (737 mg). NMR (δ (ppm), CDCl₃): ¹H (300 MHz): 8.08 – 7.96 (m, 2H), 7.50 – 7.42 (m, 4H), 2.55 (s, 3H). The spectroscopic data are consistent with those reported in the literature.³³

4-(4-(tert-butyl)phenyl)-2-chloro-6-methylpyrimidine (5): The product was synthesized by *method B* according to a similar procedure employed for compound **2**, except the 2,4-dichloro-6-methylpyrimidine (815 mg, 5 mmol, 1 equiv) and (4-(tert-butyl)phenyl)boronic

acid (980 mg, 5.5 mmol, 1.1 equiv) were used in place of **1** and phenylboronic acid and the reaction time is 24h. The crude product was purified by silica gel column chromatography (Petroleum ether to petroleum ether/AcOEt, 10:1, v/v) to give compound **5** as a pale yellow oil in 50 % yield (652 mg). NMR (δ (ppm), CDCl₃): ¹H (300 MHz): 7.77 (d, ³J_{HH} = 8.6 Hz, 2H), 7.32 – 7.23 (m, 3H), 2.32 (s, 3H), 1.15 (s, 9H); ¹³C{¹H} NMR (JMOD, 75 MHz, CDCl₃) 170.1 (C), 165.8 (C), 160.65 (C), 154.6 (C), 131.7 (C), 126.6 (CH), 125.4 (CH), 113.7 (CH), 34.3 (C), 30.6 (CH₃), 23.5 (CH₃). HRMS (ESI) *m/z* calculated for C₁₅H₁₇N₂³⁵ClNa [M + Na]⁺: 283.0972, found: 283.0970 (1 ppm).

4-methyl-6-phenyl-2-(pyridin-2-yl)pyrimidine (6): The product was synthesized by *method A* according to a similar procedure employed for compound **1**, except the compound **4** (1.0 g, 5 mmol, 1 equiv) was used in place of 2,4-dichloro-6-methylpyrimidine and the reaction time is 48h. The crude product was purified by silica gel column chromatography (Petroleum ether to petroleum ether/AcOEt, 3:7, v/v) to give compound **6** as a pale yellow oil in 72 % yield (891 mg). NMR (δ (ppm), CDCl₃): ¹H (300 MHz): 8.86 (d, ³J_{HH} = 4.0 Hz, 1H), 8.66 (d, ³J_{HH} = 7.9 Hz, 1H), 8.25 – 8.12 (m, 2H), 7.86 (td, ³J_{HH} = 7.8, ⁴J_{HH} = 1.8 Hz, 1H), 7.58 (s, 1H), 7.55 – 7.45 (m, 3H), 7.42 – 7.35 (m, 1H), 2.72 (s, 3H); ¹³C{¹H} NMR (JMOD, 75 MHz, CDCl₃) 168.8 (C), 164.1 (C), 163.5 (C), 155.5 (C), 150.1 (CH), 137.0 (C), 136.9 (CH), 130.9 (CH), 129.0 (CH), 127.4 (CH), 124.7 (CH), 124.0 (CH), 115.5 (CH), 24.9 (CH₃). HRMS (ESI) *m/z* calculated for C₁₆H₁₄N₃ [M + H]⁺: 248.1182, found: 248.1185 (1 ppm).

4-(4-(tert-butyl)phenyl)-6-methyl-2-(pyridin-2-yl)pyrimidine (7): The product was synthesized by *method A* according to a similar procedure employed for compound **1**, except the compound **5** (1.3 g, 5 mmol, 1 equiv) was used in place of 2,4-dichloro-6-methylpyrimidine. The crude product was purified by neutral Al₂O₃ column chromatography

(Petroleum ether to petroleum ether/CH₂Cl₂, 3:2, v/v) to give compound **6** as a pale yellow oil in 40% yield (607 mg). NMR (δ (ppm), CDCl₃): ¹H (300 MHz): 8.86 (d, ³J_{HH} = 4.0 Hz, 1H), 8.66 (d, J_{HH} = 7.9 Hz, 1H), 8.13 (d, ³J_{HH} = 8.5 Hz, 2H), 7.86 (td, ³J_{HH} = 7.8, 1.7 Hz, 1H), 7.54 (d, J_{HH} = 8.6 Hz, 3H), 7.42 – 7.33 (m, 1H), 2.73 (s, 3H), 1.36 (s, 3H); ¹³C{¹H} NMR (JMOD, 75 MHz, CDCl₃) 168.6(C), 164.1(C), 163.5(C), 155.6(C), 154.4(C), 150.1(CH), 136.9(CH), 134.2(C), 127.2(CH), 126.0(CH), 124.7(CH), 124.0(CH), 115.2(CH), 35.0(C), 31.3(CH₃), 24.9 (CH₃).). HRMS (ESI) *m/z* calculated for C₂₀H₂₂N₃ [M + H]⁺: 304.1808, found: 304.1811 (1 ppm).

[Pt(C[^]N[^]N)Cl] 8, Method C: A 250 ml Schlenk flask, charged with the tridentate ligand **2** (75 mg, 0.3 mmol, 1 equiv) and K₂PtCl₄ (125 mg, 0.3 mmol, 1 equiv) was degassed and back-filled with nitrogen three times. Then glacial acetic acid (60 ml) was introduced into the reaction flask by syringe. The reaction mixture was stirred under nitrogen protection under reflux for 72 h. The precipitate was filtered off and washed subsequently with water, methanol and diethyl ether. The product **8** was obtained and used without further purification as red powder in 95 % yield (136 mg). HRMS (ESI) *m/z* calculated for C₁₆H₁₂N₃³⁵ClNa¹⁹⁵Pt [M + Na]⁺: 499.0259, found: 499.0259 (0 ppm). Anal. Calcd. for C₁₆H₁₂N₃ClPt·1H₂O: C, 38.84; H, 2.85; N, 8.49, found: C, 38.93; H, 2.46; N, 8.38.

[Pt(C[^]N[^]N)Cl] 9: The product was synthesized by *method C* according to a similar procedure employed for complex **8**, except the tridentate ligand **3** (91 mg, 0.3 mmol, 1 equiv) was used in place of ligand **2**. The product **8** was obtained as as yellow powder in yield 98 % (157 mg). HRMS (ESI) *m/z* calculated for C₂₀H₂₀N₃³⁵ClNa¹⁹⁵Pt [M + Na]⁺: 555.0886, found: 555.0887

(0 ppm). Anal. Calcd. for $C_{20}H_{20}N_3ClPt$: C, 45.08; H, 3.78; N, 7.88, found: C, 44.99; H, 3.64; N, 7.78.

[Pt(C[^]N[^]N)(C≡CC₆H₄-CHO-*p*)] 10, Method D: A mixture of [(C[^]N[^]N)PtCl] **9** (54 mg, 0.1 mmol, 1 equiv) and 4-Ethynylbenzaldehyde (40 mg, 0.3 mmol, 3 equiv) in the presence of a catalytic amount of copper(I) iodide (2 mg, 10 mol%) in degassed CH₂Cl₂ : Et₃N (10:1, v/v, 60 mL) was stirred for 15 h under a nitrogen atmosphere at 50^o C. The mixture was diluted with water, and the aqueous layer was extracted with DCM (2 × 30 mL). The separated organic phase extracts were dried over MgSO₄, filtered and the solvents were evaporated under reduced pressure. The crude product was purified by neutral Al₂O₃ column chromatography (CH₂Cl₂ to CH₂Cl₂/ AcOEt, 10:3, v/v) and recrystallized from dichloromethane/diethyl ether. The product **10** was obtained as orange powder in 76 % yield (48 mg). NMR (δ (ppm), CDCl₃): ¹H (300 MHz): 9.99 (s, 1H), 9.08 (d, ³J_{HH} = 6.1 Hz, 1H), 8.02 – 7.88 (m, 2H), 7.87 – 7.71 (m, 3H), 7.64 (s, 1H), 7.63 – 7.52 (m, 3H), 7.21 (s, 1H), 7.15 (dd, ³J_{HH} = 8.1, ⁴J_{HH} = 2.0 Hz, 1H), 2.59 (s, 3H), 1.39 (s, 9H). IR (ATR, cm⁻¹): 2090 (ν_{C≡C}), 1680 (ν_{C=O}), 1587 (ν_{C=C}), 1542 (ν_{C=N}). HRMS (ESI) *m/z* calculated for C₂₅H₁₇N₃ONa¹⁹⁵Pt [M + Na]⁺: 593.0912, found: 593.0916 (1 ppm).

[Pt(C[^]N[^]N)(C≡CC₆H₄-OCH₃-*p*)] 11: The product was synthesized by *method D* according to a similar procedure employed for complex **10**, except 4-Ethynylanisole (40 mg, 0.3 mmol) was used in place of 4-Ethynylbenzaldehyde. The product **11** was obtained as red powder in 49 % yield (31 mg). NMR (δ (ppm), CDCl₃): ¹H (300 MHz): 9.06 (d, ³J_{HH} = 5.6 Hz, 1H), 8.00 (d, ⁴J_{HH} = 1.9 Hz, 1H), 7.93 – 7.84 (m, 1H), 7.78 – 7.73 (m, 1H), 7.56 (d, ³J_{HH} = 8.1 Hz, 1H), 7.58 – 7.45 (m, 4H), 7.18 (s, 1H), 7.15 – 7.12 (m, 1H), 6.86 (d, ³J_{HH} = 8.8 Hz, 1H), 3.84 (s,

3H), 2.53 (s, 3H), 1.40 (s, 9H). **IR (ATR, cm^{-1}):** 2096 ($\nu_{\text{C}\equiv\text{C}}$), 1584($\nu_{\text{C}=\text{C}}$), 1537($\nu_{\text{C}=\text{N}}$), 1031($\nu_{\text{C}-\text{O}}$). HRMS (ESI) m/z calculated for $\text{C}_{29}\text{H}_{28}\text{N}_3\text{O}^{195}\text{Pt} [\text{M} + \text{H}]^+$: 629.1875, found: 629.1876 (0 ppm).

[Pt(C[^]N[^]N)(C \equiv CC₆H₄-CN-*p*)] **12:** The product was synthesized by *method D* according to a similar procedure employed for complex **10**, except 4-Ethynylbenzonitrile (39 mg, 0.3 mmol) was used in place of 4-Ethynylbenzaldehyde. The product **12** was obtained as yellow powder in 81 % yield (51 mg). NMR (δ (ppm), CDCl_3): ^1H (300 MHz): 9.22 (d, $^3J_{\text{HH}} = 4.6$ Hz, 1H), 8.14 – 8.08 (m, 1H), 7.98 (d, $^4J_{\text{HH}} = 1.9$ Hz, 1H), 7.94 (d, $^3J_{\text{HH}} = 7.8$ Hz, 1H), 7.73 – 7.65 (m, 2H), 7.62 – 7.51 (m, 4H), 7.31 (s, 1H), 7.18 (dd, $^3J_{\text{HH}} = 8.2$, $^4J_{\text{HH}} = 1.9$ Hz, 1H), 2.65 (s, 3H), 1.37 (s, 9H). **IR (ATR, cm^{-1}):** 2220($\nu_{\text{C}\equiv\text{N}}$), 2087 ($\nu_{\text{C}\equiv\text{C}}$), 1594 ($\nu_{\text{C}=\text{C}}$), 1542 ($\nu_{\text{C}=\text{N}}$). HRMS (ESI) m/z calculated for $\text{C}_{22}\text{H}_{14}\text{N}_4\text{Na}^{195}\text{Pt} [\text{M} + \text{Na}]^+$: 552.0756, found: 552.0761 (0 ppm).

[Pt(C[^]N[^]N)(C \equiv CC₆H₄-N(CH₃)₂-*p*)] **13:** The product was synthesized by *method D* according to a similar procedure employed for complex **10**, except 4-ethynyl-N,N-dimethylaniline (44 mg, 0.3 mmol) was used in place of 4-Ethynylbenzaldehyde. The product **13** was obtained as dark red powder in 50 % yield (33 mg). NMR (δ (ppm), CDCl_3): ^1H (300 MHz): 9.07 (d, $^3J_{\text{HH}} = 6.4$ Hz, 1H), 8.04 (d, $^3J_{\text{HH}} = 1.9$ Hz, 1H), 7.89 (td, $^3J_{\text{HH}} = 7.9$, $^4J_{\text{HH}} = 1.6$ Hz, 1H), 7.80 – 7.72 (m, 1H), 7.56 (d, $^3J_{\text{HH}} = 8.1$ Hz, 1H), 7.51 (d, $^3J_{\text{HH}} = 6.2$ Hz, 1H), 7.45 (d, $^3J_{\text{HH}} = 8.8$ Hz, 2H), 7.19 (s, 1H), 7.13 (dd, $^3J_{\text{HH}} = 8.2$, $^4J_{\text{HH}} = 2.0$ Hz, 1H), 6.72 (d, $^3J_{\text{HH}} = 8.9$ Hz, 2H), 2.98 (s, 6H), 2.52 (s, 3H), 1.41 (s, 9H). **IR (ATR, cm^{-1}):** 2098 ($\nu_{\text{C}\equiv\text{C}}$), 1584 ($\nu_{\text{C}=\text{C}}$), 1534 ($\nu_{\text{C}=\text{N}}$). HRMS (ESI) m/z calculated for $\text{C}_{30}\text{H}_{31}\text{N}_4^{195}\text{Pt} [\text{M} + \text{H}]^+$: 642.2191, found: 642.2190 (0 ppm).

Synthesis of complex [Pt(C[^]N[^]N)Cl] 14: The product was synthesized by *method C* according to a similar procedure employed for complex **8**, except the tridentate ligand **6** (75 mg, 0.3 mmol) was used in place of ligand **2**. The product **14** was obtained as yellow powder in 75 % yield (108 mg). HRMS (ESI) *m/z* calculated for C₁₆H₁₂N₃³⁵ClNa¹⁹⁵Pt M⁺: 476.0362, found: 476.0358 (1 ppm). Anal. Calcd. for C₁₆H₁₂N₃ClPt: C, 40.30; H, 2.54; N, 8.81, found: C, 40.04; H, 2.45; N, 8.56.

Synthesis of complex [Pt(C[^]N[^]N)Cl] 15: The product was synthesized by *method C* according to a similar procedure employed for complex **8**, except the tridentate ligand **7** (91 mg, 0.3 mmol) was used in place of ligand **2**. The product **15** was obtained as green (brown) powder in 72 % yield (116 mg). NMR (δ (ppm), CDCl₃): ¹H (300 MHz): 9.19 (d, ³J_{HH} = 4.8 Hz, 1H), 8.38 (d, ³J_{HH} = 8.5 Hz, 1H), 8.21 – 8.10 (m, 1H), 7.90 (s, 1H), 7.77 (t, ³J_{HH} = 7.7 Hz, 1H), 7.38 (d, ³J_{HH} = 8.5 Hz, 1H), 7.24 (s, 1H), 7.17 (d, ³J_{HH} = 8.0 Hz, 1H), 2.62 (s, 3H), 1.37 (s, 9H). HRMS (ESI) *m/z* calculated for C₂₀H₂₀N₃³⁵ClNa¹⁹⁵Pt [M+Na]⁺: 555.0886, found: 555.0887 (0 ppm).

[Pt(C[^]N[^]N)(C \equiv CC₆H₄-OCH₃-*p*)] 16: The product was synthesized by *method D* according to a similar procedure employed for complex **10**, except 4-Ethynylanisole (40 mg, 0.3 mmol) and complex **15** (54 mg, 0.1 mmol) were used in place of 4-Ethynylbenzaldehyde and complex **8**. The product **16** was obtained as orange powder in 46 % yield (29 mg). NMR (δ (ppm), CDCl₃): ¹H (300 MHz): 9.23 (d, ³J_{HH} = 5.9 Hz, 1H), 8.31 (d, ³J_{HH} = 7.9 Hz, 1H), 8.18 – 7.99 (m, 2H), 7.70 – 7.63 (m, 1H), 7.50 (d, ⁴J_{HH} = 8.3 Hz, 2H), 7.31 (d, ³J_{HH} = 8.2 Hz, 1H),

7.25 (s, 1H), 7.07 (dd, $^3J_{\text{HH}} = 8.2, 1.9$ Hz, 1H), 6.85 (d, $^3J_{\text{HH}} = 8.4$ Hz, 2H), 3.83 (s, 3H), 2.62 (s, 3H), 1.37 (s, 9H). **IR (ATR, cm^{-1}):** 2102 ($\nu_{\text{C}\equiv\text{C}}$), 1590 ($\nu_{\text{C}=\text{C}}$), 1526 ($\nu_{\text{C}=\text{N}}$) 1032 ($\nu_{\text{C}-\text{O}}$). **HRMS (ESI) m/z** calculated for $\text{C}_{29}\text{H}_{28}\text{N}_3\text{O}^{195}\text{Pt} [\text{M} + \text{H}]^+$: 629.1875, found: 629.1876 (0 ppm).

[Pt(C[^]N[^]N)(C \equiv CC₆H₄-CN-*p*)] 17: The product was synthesized by *method D* according to a similar procedure employed for complex **10**, except 4-Ethynylbenzotrile (39 mg, 0.3 mmol) and complex **15** (54 mg, 0.1 mmol) were used in place of 4-Ethynylbenzaldehyde and complex **8**. The product **17** was obtained as yellow powder in 77 % yield (48 mg). NMR (δ (ppm), CDCl_3): ^1H (300 MHz): 9.19 (d, $^3J_{\text{HH}} = 4.5$ Hz, 1H), 8.42 (d, $^3J_{\text{HH}} = 7.8$ Hz, 3H), 8.24 – 7.96 (m, 2H), 7.77 – 7.68 (m, 1H), 7.64 – 7.51 (m, 4H), 7.45 (d, $^3J_{\text{HH}} = 8.3$ Hz, 1H), 7.32 (s, 1H), 7.18 (dd, $^3J_{\text{HH}} = 8.3, 2.0$ Hz, 1H), 2.67 (s, 3H), 1.35 (s, 9H). **IR (ATR, cm^{-1}):** 2221($\nu_{\text{C}\equiv\text{N}}$), 2095 ($\nu_{\text{C}=\text{C}}$), 1591 ($\nu_{\text{C}=\text{C}}$), 1562 ($\nu_{\text{C}=\text{N}}$). **HRMS (ESI) m/z** calculated for $\text{C}_{29}\text{H}_{24}\text{N}_4\text{Na}^{195}\text{Pt} [\text{M} + \text{Na}]^+$: 646.1541, found: 646.1542 (0 ppm).

Acknowledgments

M. H. acknowledges the Région Bretagne, France and Conseil Départemental des Côtes d'Armor, France for her Ph. D. funding (MMLum project).

References

-
- ¹ a) Pashaei, B.; Karimi, S.; Shahroosvand, H.; Abbasi, P.; Pilkington, M.; Bartolotta, A.; Fresta, E.; Fernandez-Cestau, J.; Costa, R. D.; Bonaccorso, F. Polypyridyl ligands as a versatile platform for solid-state light emitting devices. *Chem. Soc. Rev.* **2019**, *48*, 5033-5139.
b) Armaroli, N.; Bolink, H. J. Eds Photoluminescent materials and electroluminescent devices;

Top Curr. Chem. Springer, **2016**, pp 1-395; c) Chi, Y.; Chou, P.-T. Transition-metal phosphors with cyclometalating ligands: fundamentals and applications. *Chem. Soc. Rev.* **2010**, *39*, 638-655; d) Choy, W. C. H. ; Chan, W. K.; Yuan, Y. Recent advances in transition metal complexes and light-management engineering in organic optoelectronic devices. *Adv. Mater.* **2014**, *26*, 5368-5399; e) Yersin, H., Ed. Highly efficient OLEDs with phosphorescent materials; Wiley-VCH: Weinheim, Germany, **2008**; f) Evans, R. C.; Douglas, P.; Winscom, C. J. Coordination complexes exhibiting room-temperature phosphorescence: evaluation of their suitability as triplet emitters in organic light emitting diodes. *Coord Chem. Rev.* **2006**, *250*, 2093-2126;

² a) Segal, M.; Baldo, M. A.; Holmes, R. J.; Forrest, S. R.; Soos, Z. G. Excitonic singlet-triplet ratios in molecular and polymeric organic materials. *Phys. Rev. B* **2003**, *68*, 075211; b) Baldo, M. A. ; O'Brien, D. F.; Thompson, M. E.; Forrest, S. R. Excitonic singlet-triplet ratio in a semiconducting organic thin film. *Phys. Rev. B* **1999**, *60*, 14422;

³ a) Mao, H-T.; Li, G.-F.; Shang, G.-G.; Wang, X.-L.; Su, Z.-M. Recent progress in phosphorescent Ir (III) complexes for nondoped organic light-emitting diodes. *Coord. Chem. Rev.* **2020**, *413*, 213283; b) Li, T.-Y.; Wu, J.; Wu, Z.-G.; Zheng, Y.-X.; Zuo, J.-L.; Pan, Y. Rational design of phosphorescent iridium (III) complexes for emission color tenability and their applications in OLEDs. *Coord Chem. Rev.* **2018**, *374*, 55-92; c) Kajjam, A. B.; Vaidyanathan, S. Structural mimics of phenyl pyridine (ppy) – substituted, phosphorescent cyclometalated homo and heteroleptic iridium (III) complexes for organic light emitting diodes – an overview. *Chem. Rec.* **2018**, *18*, 293-349.

⁴ Cebrián, C. ; Mauro, M. Recent advances in phosphorescent platinum complexes for organic light-emitting diodes. *Beilstein J. Org. Chem.* **2018**, *14*, 1458-1481.

⁵ a) Wang, S. F. ; Wei, Y.-C.; Chan, W.-H.; Fu, L.-W.; Su, B.-K.; Chen, I.-Y.; Chou, K.-J.; Chen, P.-T.; Hsu, H.-F.; Ko, C.-L.; Hung, W.-Y.; Lee, C.-S.; Chou, P.-T.; Chi, Y. Highly efficient near-infrared electroluminescence up to 800 nm using platinum (II) phosphors. *Adv. Funct. Mater.* **2020**, *30*, 2002173; b) Dragonetti, C.; Fagnani, F.; Mariotto, D.; di Biase, A.; Roberto, D.; Cocchi, M.; Fantacci, S.; Colombo, A. First member of an appealing class of cyclometalated 1,3-di-(2-pyridyl)benzene platinum (II) complexes for solution processable OLEDs *J. Mater. Chem. C* **2020**, *8*, 7873-7881; c) Moon, Y. K.; Huh, J.-S.; Kim, S.; Kim, S.; Yi, S. Y.; Kim, J.-J.; You, Y. Synthetic strategy for preserving sky-blue electrophosphorescence in square planar Pt(II) complexes. *ACS Appl. Electro. Mater.* **2020**, *2*, 604-617; d) Zhao, D.; Huang, C.-C.; Liu, X.-Y.; Song, B.; Ding, L. ; Fung, M.-K.; Fan, J. Efficient OLEDs with saturated yellow and red emission based on rigid tetradentate Pt(II) complexes. *Org. Electron.* **2018**, *62*, 542-547.

⁶ Haque, A.; Xu, L.; Al-Balushi, R. A.; Al-Suti, M. K.; Ilmi, R.; Guo, Z.; Khan, M. S.; Wong, W.-Y.; Raithby, P. R. Cyclometallated tridentate platinum(II) arylacetylides complexes : old wine in new bottles. *Chem. Soc. Rev.* **2019**, *48*, 5547-5563.

⁷ a) Nisic, F.; Colombo, A.; Dragonetti, C.; Roberto, D.; Valore, A.; Malicka, J. M.; Cocchi, M.; Freeman, G. R.; Williams, J. A. G. Platinum(II) complexes with cyclometallated 5- π -delocalized-donor-1,3-di(2-pyridyl)benzene ligands as efficient phosphors for NIR-OLEDs. *J. Mater. Chem. C* **2014**, *2*, 1791-1800; b) Cocchi, M.; Virgili, D.; Fattori, V.; Rochester, D. L.; Williams, J. A. G. N[^]C[^]N-coordinated platinum(II) complexes as phosphorescent emitters in high-performance organic emitting devices. *Adv. Funct. Mater.* **2007**, *17*, 285-289; c) Williams, J. A. G.; Beeby, A.; Davies, E. S.; Weinstein, J. A.; Wilson, C. An alternative route to highly luminescent platinum(II) complexes: cyclometalation with N[^]C[^]N-coordinating dipyritylbenzene ligands *Inorg. Chem.* **2003**, *42*, 8609-8611.

-
- ⁸ a) Lai, S.-W.; Chan, M. C.-W.; Cheung, T.-C.; Peng, S.-M.; Che, C.-M. *Inorg. Chem.* **1999**, *38*, 4046-4055; b) Constable, E. C.; Henney, R. P. G. Leese, T. A.; Tocher, D. A. Cyclometallation reactions of 6-phenyl-2,2'-bipyridine; a potential C,N,N-donor analogue of 2,2':6',2''-terpyridine. Crystal and molecular structure of dichlorobis(6-phenyl-2,2'-bipyridine)ruthenium(II) *J. Chem. Soc., Dalton Trans.* **1990**, 443-449;
- ⁹ a) Yuen, M.-Y.; Kui, S. C. F.; Low, K.-H.; Kwok, C.-C.; Chui, S. S.-Y.; Ma, C.-W.; Zhu, N.; Che, C.-M. Synthesis, photophysical and electrophosphorescent properties of fluorene-based platinum(II) complexes *Chem. Eur. J.* **2010**, *16*, 14131-13141; b) Kui, S. C. F.; Sham, I. H. T.; Cheung, C. C. C.; Ma, C.-W.; Yan, B.; Zhu, N.; Che, C.-M.; Fu, W.-F. Platinum(II) complexes with π -conjugated, naphthyl-substituted, cyclometalated ligands (RC^NN): Structure and photo- and electroluminescence. *Chem. Eur. J.* **2007**, *13*, 417-435.
- ¹⁰ Chow, P.-K.; Cheng, G.; Tong, G. S. M.; To, W.-P.; Kwong, W.-L.; Low, K.-H.; Kwok, C.-C.; Ma, C.; Che, C.-M. Luminescent pincer platinum(II) complexes with emission quantum yields up to almost unity: photophysics, photoreductive C-C bond formation, and materials applications. *Angew. Chem. Int. Ed* **2015**, *54*, 2084-2089.
- ¹¹ a) Fecková, M.; le Poul, P.; Bureš, F.; Robin-le Guen, F.; Achelle, S. Nonlinear optical properties of pyrimidine chromophores. *Dyes Pigm.* **2020**, *182*, 108659; b) Achelle, S.; Rodríguez-López, J.; Robin-le Guen, F. photoluminescence properties of aryl-, arylvinyl- and arylethynylpyrimidine derivatives. *ChemistrySelect*, **2018**, *3*, 1852-1886; c) Achelle, S.; Plé, N. Pyrimidine ring as building block for the synthesis of functionalized π -conjugated materials. *Curr. Org. Synth.* **2012**, *9*, 163-197.
- ¹² a) Bori, J.; Mahata, S.; Manivanna, V. A new route for the synthesis of 2,4-bis(2-pyridyl)-6-(pyridyl)pyrimidines: synthesis and characterization of Co(II), Ni(II) complexes of 2,4,6-tris(2-pyridyl)pyrimidine. *Inorganica Chimica Acta*, **2020**, *506*, 11950; b) Hadad, C.; Achelle,

S.; López-Solera, I.; García-Martínez, J. C.; Rodríguez-López, J. Metal cation complexation studies of 4-arylvinyl-2,6-di(pyridin-2-yl)pyrimidines : effects on the optical properties. *Dyes Pigm.* **2013**, *97*, 230-237; c) Polson, M. I. J.; Lotoski, J. A.; Johanson, K. O. ; Taylor, N. J. ; Hanan, G. S.; Hasenknopf, B.; Thouvenot, R.; Loiseau, F.; Passalacqua, R.; Campagna, S. Symmetric and asymmetric coupling of pyridylpyrimidine for the synthesis of polynucleating ligands. *Eur. J. Inorg. Chem.* **2002**, 2549-2552.

¹³ a) Shafikov, M. Z.; Tang, S.; Larsen, C.; Bodensteiner, M.; Kozhevnikov, V. N.; Edman, L. An efficient heterodinuclear Ir(III)/Pt(II) complex: synthesis, photophysics and application in light-emitting electrochemical cells. *J. Mater. Chem. C* **2019**, *7*, 10672-10682; b) Zhao, J. ; Dang, F. ; Feng, Z. ; Liu, B.; Yang, X.; Wu, Y.; Zhou, G.; Wu, Z.; Wong, W.-Y. Highly efficient electroluminescent Pt^{II} ppy-type complexes with monodentate ligands. *Chem. Commun.* **2017**, *53*, 7581-7584; c) Damm, C.; Israel, G.; Hegmann, T.; Tschierske, C. Luminescence and photoconductivity in mononuclear ortho-platinated metallomesogens. *J. Mater. Chem.* **2006**, *16*, 1808-1816.

¹⁴ a) Li, X.; Hu, J.; Wu, Y.; Li, R.; Xiao, D.; Zeng, W.; Zhang, D.; Xiang, Y.; Jin, W. Tunable luminescence of cyclometalated platinum(II) derivatives based on novel pyrimidine-contained tridentate Pt(N[^]C[^]N)Cl complexes. *Dyes Pigm.* **2017**, *141*, 188-194; b) Wang, Z. ; Turner, E.; Mahoney, V.; Madakuni, S.; Groy, T.; Li, J. Facile synthesis and characterization of phosphorescent Pt(N[^]C[^]N)X complexes *Inorg. Chem.* **2010**, *49*, 11276-11286.

¹⁵ Hadad, C.; Achelle, S.; García-Martínez, J. C.; Rodríguez-López, J. 4-Arylvinyl-2,6-di(pyridine-2-yl)pyrimidines: synthesis and optical properties. *J. Org. Chem.* **2011**, *76*, 3837-3845.

¹⁶ Klikar, M.; Le Poul, P.; Růžička, A.; Pytela, O.; Barsella, A.; Dorkenoo, K. D.; Robin-le Guen, F.; Bureš, F.; Achelle, S. Dipolar NLO Chromophores Bearing Diazine Rings as π -Conjugated Linkers. *J. Org. Chem.* **2017**, *82*, 9435-9451.

¹⁷ a) Schomaker, J. M.; Delia, T. J. Arylation of Halogenated Pyrimidines via a Suzuki Coupling Reaction. *J. Org. Chem.* **2001**, *66*, 7125-7128. b) Fecková, M.; Le Poul, P.; Robin-le Guen, F.; Roisnel, T.; Pytela, O.; Klikar, M.; Bureš, F.; Achelle, A.; 2,4-Distyryl- and 2,4,6-Tristyrylpyrimidines: Synthesis and Photophysical Properties, *J. Org. Chem.* **2018**, *83*, 11712-11726.

¹⁸ Vezzu, D. A. K.; Ravindranathan, D.; Garner, A. W.; Bartolotti, L.; Smith, M. E.; Boyle, P. D.; Huo, S. Highly Luminescent Tridentate N⁴C⁶N Platinum(II) Complexes Featured in Fused Five Six-Membered Metallacycle and Diminishing Concentration Quenching. *Inorg. Chem.* **2011**, *50*, 8261-8273.

¹⁹ Lu, W.; Mi, B.-X.; Chan, M. C. W.; Zheng, Hui, Z.; Che, C.-M.; Zhu, N.; Lee, S.-T. Light-Emitting Tridentate Cyclometalated Platinum(II) Complexes Containing σ -Alkynyl Auxiliaries: Tuning of Photo- and Electrophosphorescence. *J. Am. Chem. Soc.* **2004**, *126*, 4958-4971.

²⁰ a) Liu, R.; Chang, J.; Xiao, Q.; Li, Y.; Chen, H.; Zhu, H. The synthesis, crystal structure and photophysical properties of mononuclear platinum(II) 6-phenyl-[2,2']bipyridynyl acetylide complexes. *Dyes Pigments*, **2011**, *88*, 88-94; b) Qiu, D.; Wu, J.; Xie, Z.; Cheng, Y.; Wang, L. Synthesis, photophysical and electrophosphorescent properties of mononuclear Pt(II) complexes with arylamine functionalized cyclometalating ligands. *J. Organomet. Chem.*, **2009**, *694*, 737-746.

²¹ a) Fleetham, T.; Golden, J. H.; Idris, M.; Hau, H.-M.; Sylvinson, D.; Ravinson, M.; Djurovich, P. I.; Thompson, M. E. Tuning State Energies for Narrow Blue Emission in

Tetradentate Pyridyl-Carbazole Platinum Complexes. *Inorg. Chem.* **2019**, *58*, 12348–12357;

b) Beto, C. C.; Yang, Y.; Zeman IV, C. J.; Ghiviriga, I.; Schanze, K. S.; Veige, A. S. Cu-Catalyzed Azide-Pt-Acetylide Cycloaddition: Progress toward a Conjugated Metallopolymer via iClick. *Organometallics*, **2018**, *37*, 4545-4550.

²² a) Li, K.; Tong, G. S. M.; Wan, Q.; Cheng, G.; Tong, W.-Y.; Ang, W.-H.; Kwong, W.-L.; Che, C.-M. Highly phosphorescent platinum(II) emitters: photophysics, materials and biological applications. *Chem. Sci.*, **2016**, *7*, 1653-1673; b) Haque, A.; Xu, L.; Al-Balushi, R. A.; Al-Suti, M. K.; Ilmi, R.; Guo, Z.; Khan, M. S.; Wong, W.-Y.; Raithby, P. R. Cyclometallated tridentate platinum(II) arylacetylide complexes: old wine in new bottles *Chem. Soc. Rev.*, **2019**, *48*, 5547-5563; c) Hagui, W.; Cordier, M.; Boixel, J.; Soulé, J.-F. Access to functionalized luminescent Pt(II) complexes by photoredox-catalyzed Minisci alkylation of 6-aryl-2,2'-bipyridines. *Chem. Commun.*, **2021**, *57*, 1038-1041.

²³ Lu, W.; Mi, B.-X.; Chan, M. C. W.; Hui, Z.; Che, C.-M.; Zhu, N.; Lee, S.-T. Light-emitting tridentate cyclometalated platinum(II) complexes containing σ -alkynyl auxiliaries: tuning of photo- and electrophosphorescence. *J. Am. Chem. Soc.*, **2004**, *126*, 4958-4971.

²⁴ a) Maisuls, I.; Wang, C.; Suburu, M. E. G.; Wilde, S.; Daniliuc, C.-G.; Brunink, D.; Dolsinis, N. L.; Ostendorp, S.; Wilde, G.; Kusters, J.; Resch-Genger, U.; Stassert, C. A.; Ligand-controlled and nanoconfinement-boosted luminescence employing Pt(II) and Pd(II) complexes: from color-tunable aggregation-enhanced dual emitters towards self-referenced oxygen reporters. *Chem. Sci.*, **2021**, *12*, 3270-3281; b) Ko, C.-L.; Hung, W.-Y.; Chen, P.-T.; Wang, T.-H.; Hsu, H.-F.; Liao, J.-L.; Ly, K.-T.; Wang, S. F.; Yu, C.-H.; Liu, S.-H.; Lee, G.-H.; Tai, W.-S.; Chou, P.-T.; Chi, Y. Versatile Pt(II) pyrazolate complexes: emission tuning via interplay of chelate designs and stacking assemblies. *ACS Appl. Mater. Interfaces* **2020**, *12*, 16679-16690.

²⁵ Demas, J. N.; Crosby, G. A. The measurement of photoluminescence quantum yields. A review *J. Phys. Chem.*, **1971**, *75*, 991-1024.

²⁶ Gaussian 16, Revision C.01, Frisch, M. J.; Trucks, G. W.; Schlegel, H. B.; Scuseria, G. E.; Robb, M. A.; Cheeseman, J. R.; Scalmani, G.; Barone, V.; Petersson, G. A.; Nakatsuji, H.; Li, X.; Caricato, M.; Marenich, A. V.; Bloino, J.; Janesko, B. G.; Gomperts, R.; Mennucci, B.; Hratchian, H. P.; Ortiz, J. V.; Izmaylov, A. F.; Sonnenberg, J. L.; Williams-Young, D.; Ding, F.; Lipparini, F.; Egidi, F.; Goings, J.; Peng, B.; Petrone, A.; Henderson, T.; Ranasinghe, D.; Zakrzewski, V. G.; Gao, J.; Rega, N.; Zheng, G.; Liang, W.; Hada, M.; Ehara, M.; Toyota, K.; Fukuda, R.; Hasegawa, J.; Ishida, M.; Nakajima, T.; Honda, Y.; Kitao, O.; Nakai, H.; Vreven, T.; Throssell, K.; Montgomery, J. A., Jr.; Peralta, J. E.; Ogliaro, F.; Bearpark, M. J.; Heyd, J. J.; Brothers, E. N.; Kudin, K. N.; Staroverov, V. N.; Keith, T. A.; Kobayashi, R.; Normand, J.; Raghavachari, K.; Rendell, A. P.; Burant, J. C.; Iyengar, S. S.; Tomasi, J.; Cossi, M.; Millam, J. M.; Klene, M.; Adamo, C.; Cammi, R.; Ochterski, J. W.; Martin, R. L.; Morokuma, K.; Farkas, O.; Foresman, J. B.; Fox, D. J. Gaussian, Inc., Wallingford CT, 2016.

²⁷ a) Perdew, J. P.; Burke, K.; Ernzerhof, M. Generalized Gradient Approximation Made Simple. *Phys. Rev. Lett.* **1996**, *77*, 3865-3868. b) Perdew, J.P.; Burke, K.; Ernzerhof, M. Generalized Gradient Approximation Made Simple (errata). *Phys. Rev. Lett.* **1997**, *78*, 1396-1396. c) Adamo, C.; Barone, V. Toward reliable density functional methods without adjustable parameters: The PBE0 model. *J. Chem. Phys.* **1999**, *110*, 6158-6169.

²⁸ a) Schaefer, A.; Horn, H.; Ahlrichs, R. Fully optimized contracted Gaussian basis sets for atoms Li to Kr. *J. Chem. Phys.* **1992**, *97*, 2571-2577; b) Schaefer, A.; Huber, C.; Ahlrichs, R. Fully optimized contracted Gaussian basis sets of triple zeta valence quality for atoms Li to Kr. *J. Chem. Phys.* **1994**, *100*, 5829-5835.

-
- ²⁹ a) Cossi, M.; Barone, V.; Cammi, R.; Tomasi, J. Ab initio study of solvated molecules: A new implementation of the polarizable continuum model. *Chem. Phys. Lett.* **1996**, *255*, 327-335. (b) Barone, V.; Cossi, M.; Tomasi, J. A new definition of cavities for the computation of solvation free energies by the polarizable continuum model. *J. Chem. Phys.* **1997**, *107*, 3210-3221.
- ³⁰ S. I. Gorelsky, S. I. AOMix: program for molecular orbital analysis, *York University, Toronto*, 1997.
- ³¹ Glendening, E.D.; Badenhoop, J. K.; Reed, A. E.; Carpenter, J. E.; Bohmann, J. A.; Morales, C. L.; Weinhold, F. 2013, NBO 6.0; Theoretical Chemistry Institute, University of Wisconsin, Madison, WI, <http://nbo6.chem.wisc.edu>.
- ³² Dennington, R.; Keith, T.; Millam, J.; Eppinnett, K.; Hovell, W. L.; Gilliland, R. GaussView, 2009.
- ³³ Kamal, R.; Kumar, R.; Kumar, V.; Kumar, V.; Bansal, K. K.; Sharma, P. C. Synthesis, anthelmintic and antimicrobial evaluation of new 2-arylidene-1-(4-methyl-6-phenylpyrimidin-2-yl)hydrazines *ChemistrySelect* **2019**, *4*, 713-717.